

A SEMI-EMPIRICAL STUDY OF THE THERMODYNAMICS OF THE DIELS-
ALDER REACTIONS OF N, P, O, AND S SUBSTITUTED FIVE MEMBERED
HETEROCYCLIC AROMATIC RINGS WITH ACROLEIN.

by

Tarek H. Musslimani

Submitted in partial Fulfillment of the Requirements

for the Degree of

Master of Science

in the

Chemistry

Program

YOUNGSTOWN STATE UNIVERSITY

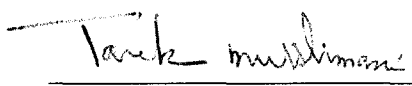
MAY, 2004

A SEMI-EMPIRICAL STUDY OF THE THERMODYNAMICS OF THE DIELS-ALDER REACTIONS OF N, P, O, AND S SUBSTITUTED FIVE MEMBERED HETEROCYCLIC AROMATIC RINGS WITH ACROLEIN.


Tarek H. Musslimani

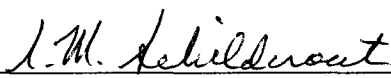
I hereby release this thesis to the public. I understand this thesis will be housed at the Circulation Desk of the University library and will be available for public access. I also authorize the University or other individuals to make copies of this thesis as needed for scholarly research.

Signature:

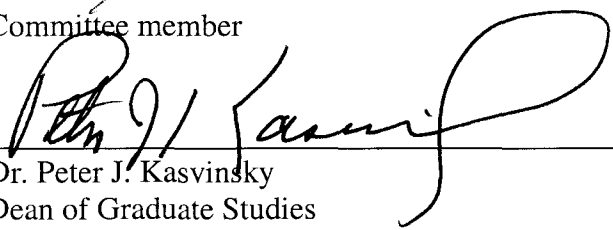

Tarek H. Musslimani
Date 3/16/04

Approvals:


Dr. Howard Mettee
Thesis Advisor
Date 3/16/04


Dr. Steven Schildcrout
Committee member
Date 3/16/04


Dr. Allen Hunter
Committee member
Date 3/17/04


Dr. Peter J. Kasvinsky
Dean of Graduate Studies
Date 3/17/04

Abstract

A semi-empirical study of the effect of substituent on the HOMO-LUMO energies of the 3,4 disubstituted 5-membered heterocyclic aromatic compounds, on the equilibrium constants of the Diels-Alder reaction of N, P, O and S substituted heterocyclic 5-membered aromatic rings with acrolein, and on the enthalpy change of the reactions, gave results in accordance with the familiar Diels-Alder reaction. A linear correlation was found between E_{HOMO} and E_{LUMO} of the diene and σ_{p} and σ_{m} of the Hammett equation. The log of the equilibrium constant calculated from the computed enthalpy and entropy of the reactions at 298 K, and the reaction enthalpy itself, also correlated with σ_{p} and σ_{m} , as expected for linear free energy relationships.

Acknowledgements

I would like to thank Professor Howard Mettee for supervising this project and for his devoted guidance during the period of this project, especially his revisions and corrections of the paper, research proposal, and the thesis which made them successful. In addition I would like to thank Professor Steven Schildcrout and Professor Allen Hunter for being on my thesis committee. Special thanks are also due to the Chemistry Department at YSU for the financial support during the summer, which made it possible to continue work on this project.

Table of Contents

	Page
Title page	i
Signature page	ii
Abstract	iii
Acknowledgements	iv
Table of Contents	v
List of Tables	vi
List of Figures	viii
List of Symbols and Abbreviations	x
I) Introduction	1
II) Literature review	2
IIA) Mechanism of the Diels-Alder reaction	3
IIB) Normal and inverse electron demand	5
IIC) Kinetic vs thermodynamic control	7
IID) Lewis acid catalyzed Diels-Alder reaction	9
III) Computational methods	11
IIIA) Molecular mechanics	11
IIIB) Hartree-Fock model	12
IIIC) Density Functional Theory	15
IIID) Semi-empirical methods	20
IIIE) Definition and meaning of the standard deviation	24
IIIF) Choice of substituent parameter	25

Table of Contents (cont'd)

IV) Results and discussion	26
IVA) Correlation between experimental and computational data	26
IVB) Effect of substituent on the energy levels of the HOMO and LUMO of the diene.	27
IVC) Correlation between E_{HOMO} and E_{LUMO} with σ_{p} and σ_{m}	29
IVD) Correlation between log of the equilibrium constant and σ_{p} and σ_{m} of Hammett.	38
IVE) Correlation between the enthalpy of the Diels-Alder reaction between 3,4 disubstituted furan, thiophene, pyrrole and phosphole vs σ_{p} and σ_{m} .	44
V) Synopsis of kinetic work	50
VI) Future work	55
VII) Conclusions	56
VIII) Bibliography	58

List of Tables

	Page
1) Experimental and calculated values of reaction enthalpy of the Diels-Alder reactions using semi-empirical, Density Functional and Hartree-Fock methods.	26
2) Types of Diels-Alder reactions.	27
3) Calculated E_{HOMO} and E_{LUMO} values for 3,4 di substituted pyrrole, furan thiophene and phosphole using AM1 and PM3.	28
4) A least square summary of the plots of E_{HOMO} and E_{LUMO} of the dienes vs σ_{p} and σ_{m} .	37
5) A least square summary of $\log K_{\text{e}}$ vs σ_{p} and σ_{m} of diene substituents.	39
6) $\log K_{\text{e}}$ values of endo reactions between 3,4 disubstituted furan, thiophene pyrrole and phosphole with acrolein.	40
7) A least square summary of the plots of the enthalpy of endo reactions between 3,4 disubstituted furan with acrolein vs σ_{p} and σ_{m} .	45
8) A least square summary of the plots of the enthalpy of the endo reactions between 3,4 disubstituted phosphole with acrolein vs σ_{p} and σ_{m} .	45
9) A least square summary of the plot of enthalpy of endo reaction between 3,4 disubstituted pyrrole with acrolein vs σ_{p} and σ_{m} .	46
10) A least square summary of the plot of enthalpy of endo reaction between 3,4 disubstituted thiophene with acrolein vs σ_{p} and σ_{m} .	46
11) Activation energy(kcal/mol) of endo Diels-Alder reaction of 3,4 disubstituted furan with acrolein.	50
12) Activation energy(kcal/mol) of endo Diels-Alder reaction of 3,4 disubstituted thiophene with acrolein.	51
13) Activation energy(kcal/mol) of endo Diels-Alder reaction of 3,4 disubstituted pyrrole with acrolein.	51
14) Activation energy(kcal/mol) of endo Diels-Alder reaction of 3,4 disubstituted phosphole with acrolein.	52

List of Tables (Cont'd)

- 15) A least square summary of the plots of the activation energy of the Diels-Alder reaction of 3,4 disubstituted furan, thiophene, pyrrole, and phosphole vs σ_R of Taft equation. 52
- 16) A least square summary of the plots of the activation energy of the Diels-Alder reactions of furan, thiophene, pyrrole, and phosphole with acrolein vs ($E_{HOMO} - E_{LUMO}$). 52

List of Figures

	Page
1) Plot of E(HOMO) of the designated furan system.	29
2) Plot of E(HOMO) of the designated furan system.	30
3) Plot of E(HOMO) of the titled phosphole system.	30
4) Plot of E(HOMO) of the noted phosphole system.	31
5) Plot of E(HOMO) of the designated thiophene system.	31
6) Plot of E(HOMO) of the noted thiophene system.	32
7) Plot of E(HOMO) of the designated pyrrole system.	32
8) Plot of E(HOMO) of the titled pyrrole system.	33
9) Plot of E(LUMO) of the titled furan system.	33
10) Plot of E(LUMO) of the referenced furan system.	34
11) Plot of E(LUMO) of the captioned phosphole system.	34
12) Plot of E(LUMO) of the titled phosphole system.	35
13) Plot of E(LUMO) of the referenced thiophene system.	35
14) Plot of E(LUMO) of the referenced thiophene system.	36
15) Plot of E(LUMO) of the captioned pyrrole system.	36
16) Plot of E(LUMO) of the titled pyrrole system.	37
17) Plot of $\log K_e$ of the titled phosphole system.	41
18) Plot of $\log K_e$ of the referenced phosphole system.	41
19) Plot of $\log K_e$ of the titled thiophene system.	42

List of Figures (cont'd)

20) Plot of $\log K_e$ of the referenced pyrrole system.	42
21) Plot of $\log K_e$ of the captioned pyrrole system.	43
22) Plot of $\log K_e$ of the titled furan system.	43
23) Plot of $\log K_e$ of the referenced furan system.	44
24) Plot of ΔH of the titled pyrrole system.	47
25) Plot of ΔH of the referenced thiophene system.	47
26) Plot of ΔH of the captioned thiophene system.	48
27) Plot of ΔH of the titled phosphole system.	48
28) Plot of ΔH of the titled furan system.	49
29) Plot of ΔH of the referenced furan system.	49
30) Energy profile for the endo retro-Diels-Alder reaction of 3,4 disubstituted furan with acrolein.	53
31) Plot of the activation energy E_a of endo retro-Diels-Alder reaction of 3,4 disubstituted furan with acrolein vs σ_R of Taft equation.	54

List of Symbols and abbreviations

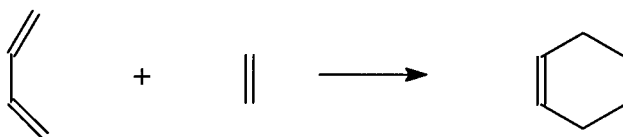
AM1	Austin model 1, a semi-empirical method
B3LYP	A density functional method due to Lee, Yang, and Parr
DFT	Density functional theory
EWG	Electron withdrawing group
HF	Hartree-Fock method
HOMO	Highest occupied molecular orbital
LDA	Local density approximation
LUMO	Lowest unoccupied molecular orbital
MNDO	Modified neglect of diatomic overlap
PM3	Parametrized model 3, a semi-empirical method
ΔG^0	Standard free energy change between reactants and products
ΔH^0	Standard enthalpy change between reactants and products
ΔS^0	Standard entropy change between reactants and products
ΔG^\ddagger	Free energy change between reactants and transition state
ΔH^\ddagger	Enthalpy change between reactants and transition state
ΔS^\ddagger	Entropy change between reactants and transition state
R	Universal gas constant
k	Boltzmann constant

List of Symbols and abbreviations (cont'd)

h	Planck constant
STO-3G	Slater type orbitals in terms of three gaussians
3-21G	Split valence basis set using three gaussians for inner shell orbitals
6-21G	Split valence basis set using six gaussians for inner shell orbitals
6-31G*	Split valence basis set with d-orbitals
6-31G**	Split valence basis set 6-31G** with additional p-orbitals
K_e	Equilibrium constant between reactants and products
K^\ddagger	Equilibrium constant between reactants and transition state
σ_m	Hammett substituent parameter for electron donating or withdrawal in meta position of benzoic acid
σ_p	Hammett substituent parameter for electron donating or withdrawal in para position of benzoic acid
σ_m^2	Variance in slope of straight line, m , fitting experimental points

I) Introduction

The Diels-Alder reaction is one of the most well known pericyclic reactions. It was discovered in the 1920s by Otto Diels and Kurt Alder in Germany.¹ After its discovery, it became one of the powerful tools in synthetic organic chemistry.² A Nobel prize was given in 1950 for its discovery. It requires a diene and a dienophile which react under thermal conditions. It is believed to take place in a concerted manner in which bond breaking and bond formation occur simultaneously without forming intermediates.

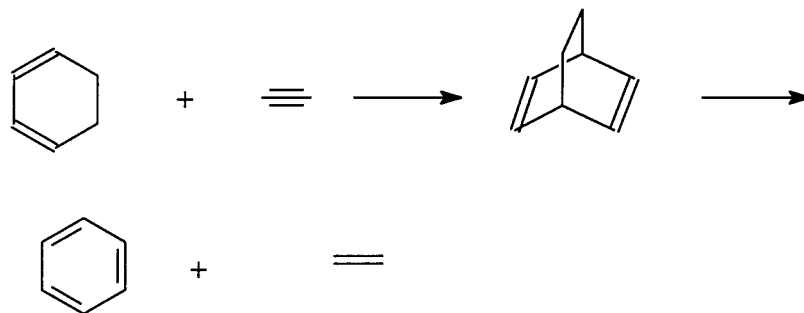


Scheme 1

Little experimental kinetic and thermodynamic work has been done on the Diels-Alder reaction of S, O, N and P substituted heterocyclic 5-membered aromatic rings with dienophiles under catalyzed and noncatalyzed conditions. Synthetic work on the Diels-Alder reaction of the foregoing heterocyclic compounds and various dienophiles has been reported with thiophene³, furan⁴, pyrrole⁵ and phosphole.⁶

II) Literature review

Mele and Huybrechts⁷ investigated the selectivity-reactivity correlations for thermal Diels-Alder reactions of cyclohexa-1,3-diene with substituted ethenes in the gas phase and found that Selectivity-Reactivity correlations support a biradical pathway for the gas phase reaction except when the substituent on the ethene is a carbonyl group.⁸ The kinetics and mechanism of the reaction of acetylene with cyclohexa-1,3-diene was investigated by Huybrechts *et al.*⁹ who found that the products of the cycloaddition reaction are ethene and benzene and not the bicyclic compound. In this case the normal bicyclic adduct rearranges, as sometimes occurs due to low kinetic barrier and extra product stability (See Scheme 2).



Scheme 2

Cetiviela *et al.*¹⁰ investigated the correlation between the log of the rate constant of the Diels-Alder reaction between cyclopentadiene and methyl (E)- α -cyano-cinnamate at 25⁰ C vs the solvophobicity parameter S_p and found a linear correlation between them. Wasserman investigated the kinetic and thermodynamic parameters of several Diels-Alder reactions in the gas and condensed phase and collected these data for the enthalpies and activation energies of these reactions in a book.¹¹

Jursic¹² studied the reactivity of furan, pyrrole, and thiophene theoretically using semiempirical and hybrid density functional theories and found that furan is a good diene for the Diels-Alder reaction. He found also that thiophene is an unreactive diene, and pyrrole fell somewhere between the other two in reactivity.

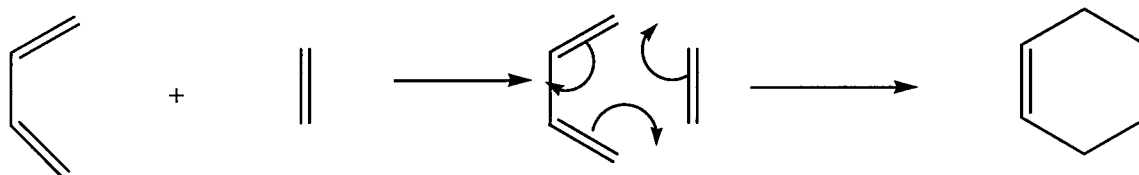
Vijaya *et al.*¹³ investigated theoretically the Diels-Alder reaction between cyclic five-membered dienes (CH)₄X, (X= CH₂, SiH₂, O, NH, PH and S) and acetylene at hybrid density functional and semiempirical levels. He found that the reaction of these five-membered rings with acetylene shows higher activation energy and higher exothermicity compared to those with ethylene dienophiles.

Experimental kinetic and thermodynamic works have been done on different Diels-Alder reactions¹⁴, however, such studies of the above heterocyclic compounds with acrolein have not. We have chosen acrolein as a dienophile because its reaction can give either endo or exo products, its reaction can be subject to Lewis acid catalysis, and it did not show the selectivity-reactivity correlation as seen by Mele and Huybrechts so we wondered why. The importance of the study is not only that it gives more insight on the behaviour of these heterocyclic compounds as dienes in the Diels-Alder reactions, but also that it reveals what level of theory and what model conditions are appropriate to describe the thermodynamic and kinetic behavior of these systems.

IIA) Mechanism of the Diels-Alder reaction

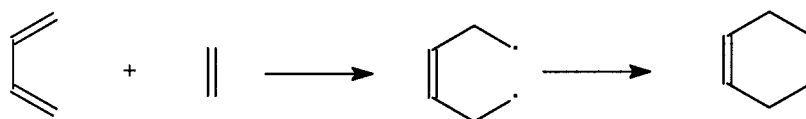
In 1935, the first mechanism for a Diels-Alder reaction was proposed by A. Wasserman¹⁵ who postulated a concerted transition state for the reaction. Later, three mechanisms were considered for the Diels-Alder reaction. 1) The concerted Mechanism A is postulated to occur without development of charge in the transition state and a

synchronous formation and breaking of bonds. (Scheme 3)



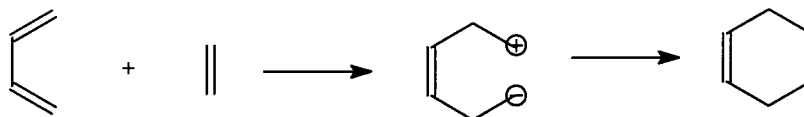
Scheme 3: Mechanism A

Mechanism B postulates a diradical development at the transition state. This hypothesis was supported by Littman and by Kistiakowsky and Mears.¹⁶ (Scheme 4)



Scheme 4: Mechanism B, diradical species intermediate.

2) Mechanism C postulates a charge-separated, zwitterion-like species in the transition state (Scheme 5)



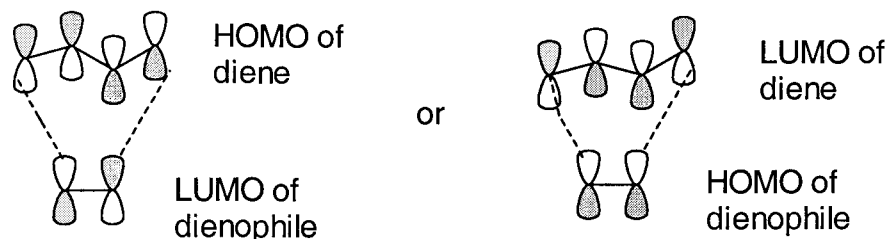
Scheme 5: Mechanism C, bipolar charged species intermediate.

The current belief is that the Diels-Alder reaction takes place via Mechanism A, the concerted synchronous mechanism. The evidence for this belief is that the Diels-Alder reaction is stereospecific, and the development of charge or diradical intermediates

in the transition state would destroy this stereospecificity.

IIB) Normal and inverse electron demand

The Diels-Alder reaction is governed by HOMO-LUMO interactions¹⁷ like many other electrocyclic reactions. (Scheme 6)



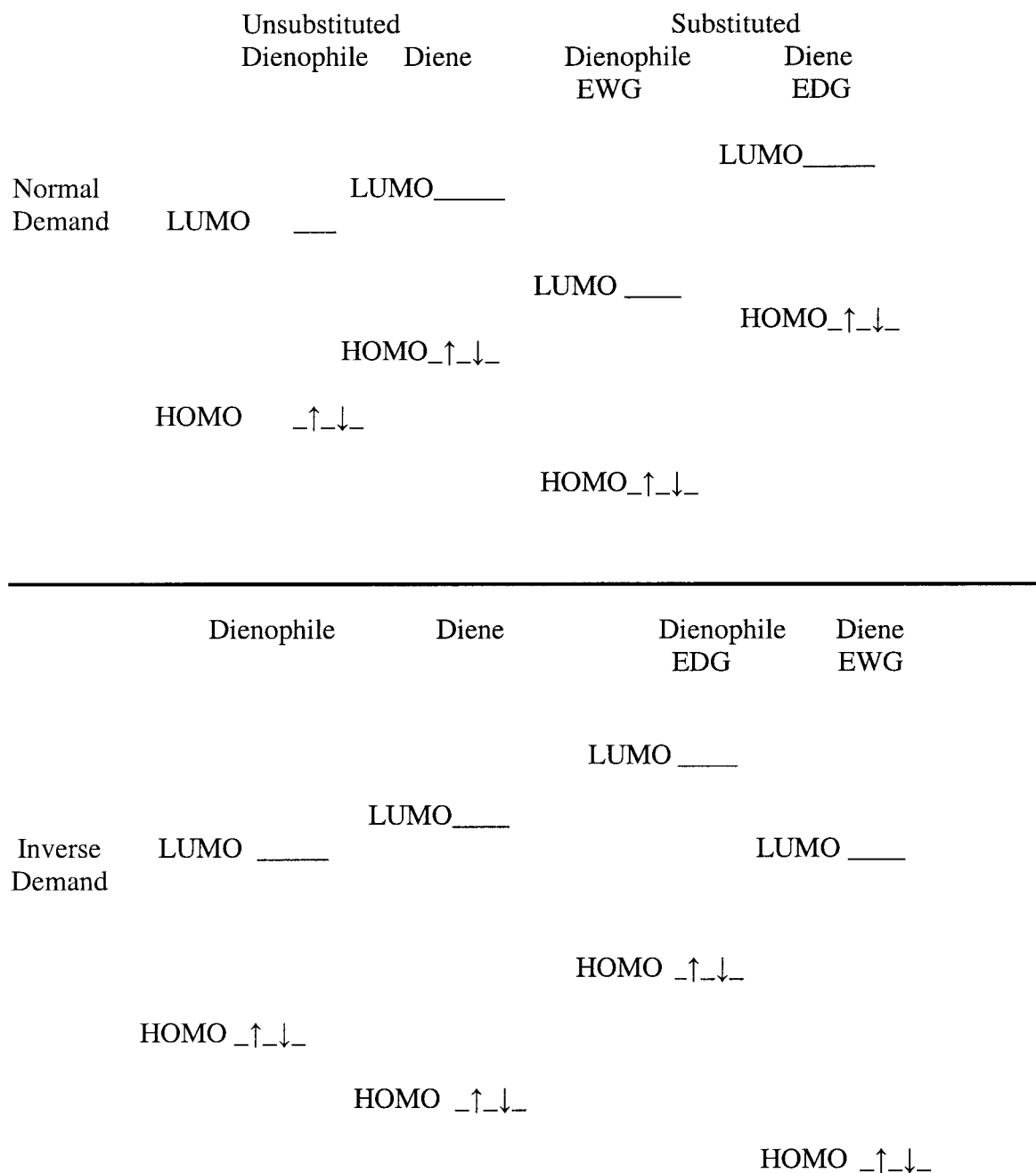
Scheme 6: Interaction of HOMO of diene and LUMO of dienophile and interactions of HOMO dienophile and LUMO of diene.

Normal electron demand¹⁸ (Scheme 7) is defined as, when electron donating groups (EDG) are on the diene and electron withdrawing groups (EWG) are on the dienophile. It predicts, and experiments show, that Diels-Alder reactions are accelerated under these conditions. The electron rich substituent effect is to raise the energy of the orbitals of the diene and lower the energy of the orbitals of the dienophile (Scheme 7). This brings the HOMO of the diene and the LUMO of the dienophile into closer energetic proximity. In turn, this lowers the activation energy by using the HOMO of the diene as the originating frontier orbital.

Inverse electron demand¹⁹ is defined when there are EDG on the dienophile and EWG on the diene. This condition destabilizes the HOMO (and other) orbitals of the dienophile and stabilizes the LUMO (and other) orbitals of the diene, since in this case the HOMO of the dienophile is the frontier orbital. The activation energy is again

lowered, as before, but in this case by using the opposite HOMO/LUMO pair of orbitals.

It should be noted that in the normal case the HOMO of the diene lies above that of the dienophile, which defines the frontier donor orbital as that of the diene. In the inverse case, the HOMO of the diene lies below that of the dienophile. This difference

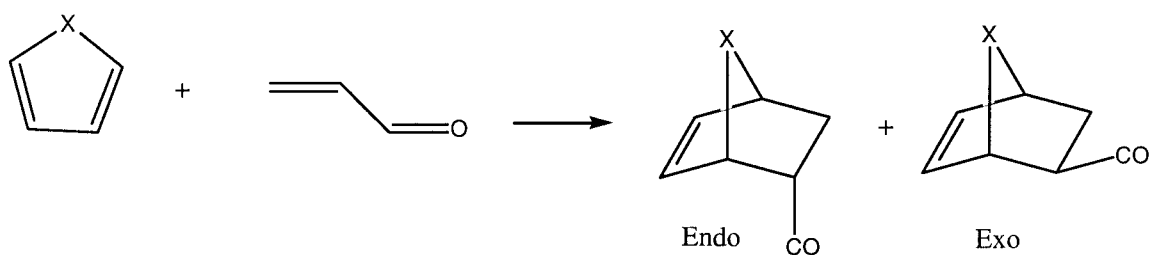


Scheme 7: Substituent effects on normal and inverse electron demands showing lower barriers for the substituted cases.

dictates whether normal or inverse substituent effects will be observed. Normal electron demand reactions tend to predominate.

IIC) Kinetic vs thermodynamic control

Cyclic dienes react with α, β unsaturated ketones to give a mixture of both exo and endo products. (Scheme 8). For our systems X = O, S, NH, and PH for furan, thiophene, pyrrole, and phosphole respectively.



Scheme 8

The endo product is kinetically favored due to a lower activation energy E_a while the exo product is thermodynamically favored due to the larger negative ΔH^0 of the reaction.

The endo product is favored over the exo product in the transition state due to secondary orbital overlap which does not exist in the exo transition state. The energy barrier E_a for the endo transition state is lower than for the exo, while the exothermicity is greater for the exo product. Reasonable transition state structures suggest that the diene and dienophile are in parallel planes.²⁰

The equilibrium constant for the reaction is a thermodynamic property of the reactants and products and is a function of the Gibbs free energy, ΔG^0 , according to the following equation:

$$\Delta G^0 = -RT \ln K_e$$

where R is the gas constant and T is the absolute temperature and K_e is the equilibrium constant.

In general, $\Delta G > 0$ refers to a nonspontaneous reaction;

$\Delta G = 0$ refers to an equilibrium state of the reaction;

$\Delta G < 0$ refers to a spontaneous reaction;

ΔG^0 is related to the standard entropy and enthalpy of the reaction by the following equation. The superscript (⁰) refers to the standard conditions at 298K and 1 bar pressure.

$$\Delta G^0 = \Delta H^0 - T\Delta S^0$$

The rate constant of a reaction is a kinetic property and is related to the activation energy by the Arrhenius equation:

$$\ln k_1 = \ln A - E_a/RT$$

where k_1 is the rate constant and A is a frequency factor. The Eyring equation gives a relation which links the rate constant and the equilibrium constant between the reactants and transition state:

$$k_1 = (kT/h)K^\ddagger$$

where k is Boltzmann constant, h is Planck constant and K^\ddagger is the equilibrium constant between reactants and transition state. The superscript (\ddagger) refers to this equilibrium. The free energy of activation is related to the enthalpy of activation and entropy of activation by the equation below:

$$\Delta G^\ddagger = \Delta H^\ddagger - T\Delta S^\ddagger$$

The activation energy E_a is related to the enthalpy of activation ΔH^\ddagger by the following equation:

$$E_a = \Delta H^\ddagger + 2RT$$

We can express the equilibrium constant using the expression for the free energy of activation by the equation below:

$$\ln K^\ddagger = -\Delta H^\ddagger/RT + \Delta S^\ddagger/R$$

The rate constant can then be written using the Eyring equation as follows.

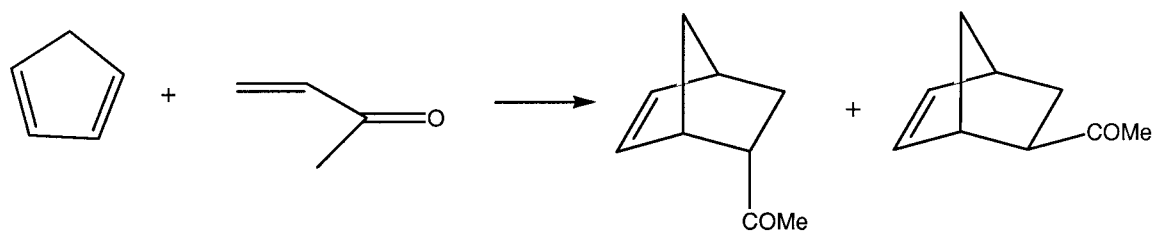
$$\ln k_1 = \ln(kT/h) - \Delta H^\ddagger/RT + \Delta S^\ddagger/R$$

IID) Lewis acid catalyzed Diels-Alder reaction

Yates and Eaton²¹ were the first to report a Lewis acid catalyzed Diels-Alder reaction. The main effect of the Lewis acid is on the LUMO of the dienophile of

α , β unsaturated ketones. The Lewis acid binds to the oxygen through its lone pair and makes the π system more electron deficient. This stabilizes the LUMO of the dienophile bringing it closer in energy to the HOMO of the diene. The consequences of the Lewis acid effect are to reduce the temperature requirement of the reaction and to increase the endo selectivity of the product. The reaction of cyclopentadiene and methylacrylate gives predominantly the endo product under noncatalyzed conditions. The yield of the endo product is still higher if Lewis acids are used.²¹ (Scheme 9)

Scheme 9: Diels-Alder reaction of cyclopentadiene and methylvinylketone.



	Temperature	Endo %	Exo %
Without AlCl ₃	0 ⁰ C	88%	12%
With AlCl ₃	0 ⁰ C	96%	4%
With AlCl ₃	-80 ⁰ C	99%	1%

The higher selectivity of the endo product with the acid is explained by the rationale that the carbonyl carbon p-orbital coefficient in the participating LUMO is mathematically found to increase upon protonation of the oxygen. In this project the thermodynamics of the Diels-Alder reactions of N, P, O, and S substituted five membered heterocyclic compounds with acrolein is investigated. The main methods used are the semi-empirical AM1 and PM3 levels of treatment.

III) Computational methods

The HOMO and LUMO energies of the dienes were calculated using AM1 and PM3 levels, and all other calculations were done using only the PM3 level, since it was found to be more accurate when compared to experiment. The modeling system that was used is the Spartan Pro program and all the plots were done using PSI Plot. The general procedure was to construct the reactant and product molecules, followed by specifying the type of calculation (SCF, semi-empirical, etc) and the basis set of orbitals if required. The program adjusts the molecular geometry so as to minimize the energy, at which point the thermodynamic parameters (ΔH , ΔS) are generated from the moments of inertia, normal vibrational modes and coulombic effects of electrons surrounding a frozen nuclear skeleton. PSI plot not only produces graphical representations but by linear regression analysis generates the “best fit” straight line slopes and intercepts with their standard deviations. We chose to discriminate trends by comparing the magnitude of the slope of a line with the standard deviation, and not with the less informative through commonly used correlation coefficient.

IIIA) Molecular mechanics.

This method is based on the classical Hooke's law or harmonic oscillator, which treats the chemical bond between two adjacent atoms as a spring with a force constant k . The restoring force between these two atoms is proportional to the displacement from the rest position (x):

$$F = -kx$$

The potential energy of the spring is:

$$U = \frac{1}{2} kx^2$$

This method tries to reproduce experimental data using parameterization of mechanical and electronic interactions. The potential energy of the molecule is a summation of stretching, bending, torsional motions and van der Waals interactions over the molecule, in addition to charge-charge and dipole-dipole effects.

IIIB) Hartree-Fock model

Hartree Fock (HF) or *ab initio* method approximates the true many-electron wave function as a product of N single electron wave functions (Scheme 10), in determinantal form:

$$\Psi(1, 2, \dots, N) = \frac{1}{\sqrt{N!}} \begin{vmatrix} U_1(1) & U_2(1) & \dots & U_n(1) \\ U_1(2) & U_2(2) & \dots & U_n(2) \\ \vdots & \vdots & \ddots & \vdots \\ U_1(n) & U_2(n) & \dots & U_n(N) \end{vmatrix}$$

Scheme 10

where the U's are orthonormal spin orbitals and $1/\sqrt{N!}$ is a normalizing factor.

The energy of the system is obtained using the variation method, which minimizes the energy with respect to the coefficients of the orbitals. It is based on the Born-Oppenheimer approximation, which states that nuclear motion is independent of

electronic motion. Furthermore, it states that the nuclei are frozen in their equilibrium position on the time scale of the electronic motion. In the Hartree-Fock model, a Slater type orbital is used, which has the following form:

$$S_{n, l, m} = N_{(n, l)} r^{n-1} e^{-\zeta r} Y_m(\theta, \varphi)$$

Where ζ is the adjustable parameter and $Y_m(\theta, \varphi)$ are the spherical harmonics. This function is approximated using a linear combination of one to six gaussian type orbitals according to the following equation:

$$\Phi(r) = (2\alpha/\pi)^{3/4} e^{-\alpha r^{**2}}$$

The HF approximation which states that the many-electron wave function can be approximated using a multiplication of one-electron-functions follows from the assumption that the electron solutions for the many-electron molecule will closely resemble a combination of one-electronic energy solutions for the hydrogen atom. Various levels of HF theory are possible, and some selection is required depending on the system to be investigated, the accuracy desired, and the computer resources at hand.

1) Closed-shell determinantal wavefunctions

Closed shell single determinant wave functions characterize the most commonly used form of HF theory, and they are appropriate for the description of the ground states of most molecules with an even number of electrons.

2) STO-3G minimal basis set.²²

The basis set termed STO-3G consists of a minimal basis, and it uses Slater type orbitals and expands each one in terms of three gaussian functions. This is important because it approximates the Slater type functions in terms of three mathematically manageable gaussian functions. Slater type orbitals are mathematically difficult and their calculations are time consuming to perform because of the evaluation of two electron-integrals. Gaussian functions can be evaluated analytically due to the $\exp(-r^2)$ term, which is not available in Slater type orbitals (which depend on $\exp(-r)$).

3) 6-21G and 3-21G split valence basis sets.^{23, 24}

These basis sets are representations in which each outer shell orbital (except for H) is represented by two functions, one contracted and the other diffuse. In each case, the inner functions are composed of two gaussians while the outer (diffuse) functions are made up of only one gaussian. In the 6-21G basis set, each inner-shell atomic orbital ((1s) for second row atoms) is written in terms of six gaussian primitives.

4) 6-31G* basis set.

This basis uses six gaussian primitives for the core orbitals, and a three/one split pair for each s and p valence orbital and a single set of six d-functions, second order gaussians which are equivalent to one s and five d orbitals.

5) 6-31G basis set.**²⁴

This basis set has in addition to 6-31G*, a set of p orbitals which has been added to each hydrogen to allow for polarization in hydrogen bonding. The p orbitals perform

the same function for the s-valence orbital of hydrogen, as the d-orbitals do for the p valence orbitals in the second row elements.

6) 6-311G basis set.²⁴

A higher level of valence shell splitting is contained in the 6-311G basis set. As before, the inner-shell atomic orbitals are represented in terms of six gaussian primitives, but it splits the valence functions into three parts instead of two, these being written in terms of three, one and one gaussian primitives, respectively.

IIIC) Density Functional Theory

Density Functional Theory (DFT) is a technique for solving the Schrodinger equation:

$$H\Psi = E\Psi$$

where the Hamiltonian operator H is a combination of kinetic and potential energy operators, which account for the interacting electrons, the nuclear-electron attraction, coulombic repulsion of the nuclei and a final term for the exchange and correlation energy of the electrons. DFT is an accurate method for predicting the ground state energy of compounds. The idea behind DFT is to describe the interacting system of electrons by means of its charge density and not via many electron wave functions.

For the electron density, the basic variables of the system depend only on three coordinates x, y, and z rather than the 3N variables required for describing the N-electron wave function. The electron exchange correlation functionals (function of a function) are usually described as functionals, which result from operating on the electronic

density distribution.²⁶ The exchange correlation functional may be approximated using the following different techniques:

- 1) Local density approximation (LDA).
- 2) Non local extension to LDA.
- 3) Hybrid Functional Methods

The LDA functional can be regarded as an exchange correlational functional for a homogeneous electron gas. The first DFT model was put forward independently by L. H. Thomas and E. Fermi^{26c} before the introduction of Hartree-Fock theory. They simply assumed the existence of an energy functional and derived an expression for the kinetic energy based on the density of electrons, $\rho(\mathbf{r})$, in an infinite potential well. This kinetic energy functional is given by:

$$T_{TF}(\rho) = (3/10)(3\pi^2)^{2/3} \int d\mathbf{r} \rho^{5/3}(\mathbf{r})$$

This equation is one of the most important ideas of modern physics, since it is the first introduction of a Local Density Approximation.

The Thomas-Fermi energy is given as a sum of the electronic kinetic energy (T) and the electron nucleus attraction energy and the Hartree correlation energy according to the following equation:

$$E_{TF}(\rho) = T_{TF}(\rho) - Z \int d\mathbf{r} \rho(\mathbf{r})/|\mathbf{R}-\mathbf{r}| + \frac{1}{2} \int d\mathbf{r}_1 d\mathbf{r}_2 \rho(\mathbf{r}_1) \rho(\mathbf{r}_2)/|\mathbf{r}_1-\mathbf{r}_2|$$

where Z is the nuclear charge, and R is the position vector of the nucleus.

In 1964 Hohenberg and Kohn^{26c} were working together in Paris investigating the foundation of the Thomas-Fermi model. They gave proofs of two important

theorems. They considered that an electronic system with a given Hamiltonian has a ground state energy as well as a ground state wave function, which is completely determined by the minimization of the total energy as a functional of the wave function. They also assumed that the external potential, together with the number of electrons, completely determines the Hamiltonian, and that these two quantities determine all the properties of the ground state.

The first Hohenberg-Kohn theorem^{26c} states: "The external potential $v(r)$ is determined, within a trivial additive constant, by the electron density $\rho(r)$ ". Since the electron density is determined by the number of electrons, it follows that the electron density determines the wave function and thereby all of the ground state properties of the system. The proof of the theorem assumes the existence of two external potentials which differ by more than a constant, and which lead to the same ground state density. This implies the existence of two different Hamiltonians, with differing wave functions, corresponding to the same ground state electron density. The electron density determines all properties of the ground state including the total ground state energy E_{tot} , the ground state kinetic energy T , the energy of the electrons in the external potential U , and the electron-electron interaction energies W , all of these are functionals of the electron density. The total energy can therefore be written as:

$$E^0(\text{tot}) = E_{\text{tot}}(\rho^0) = T(\rho^0) + U(\rho^0) + W(\rho^0)$$

where ρ^0 denotes the true ground state electron density of the system. The first Hohenberg-Kohn theorem thus establishes the existence of the total energy functional,

but it does not provide the solution to the many body electron problem.

The second Hohenberg-Kohn theorem^{26c} provides a variational principle: "For any given non-negative trial density, $\rho(r)$, that integrates to the correct number of electrons, N , the true ground state energy $E^0(\text{tot})$ satisfies the relation":

$$E^0(\text{tot}) \leq E_{\text{tot}}[\rho(r)]$$

This provides a way (by minimization of E_{tot}) to obtain solutions for the total energy if $T(\rho)$, $U(\rho)$ and $W(\rho)$ are known functionals.

When Kohn returned to the USA from his trip to France, he continued working with his postdoctoral student L. J. Sham. There was a need to find good approximation to the unknown $T(\rho)$ and $W(\rho)$ functionals. To treat the kinetic energy better, they reintroduced non-interacting orbitals of neutral density into the problem. Using a non-interacting reference system, for which the ground state density is exactly equal to the ground state density of the fully interacting system, they succeeded in showing that any N -electron density can be uniquely decomposed into orbitals. These are called the Kohn-Sham orbitals (KS), and the expectation value of the kinetic energy operator using these orbitals is the non-interacting kinetic energy $T_s(\rho)$.

The exchange and correlation energy functional is not in general equivalent to the quantum chemical exchange and correlation. The inclusion of correlation effects in the KS orbitals makes these different from the HF-orbitals. If one would use the same orbitals in both methods, the same operator would be used for the kinetic energy, and the external potential would also be the same. The total exchange and correlation energy in the two descriptions would therefore be the same.

When the Hohenberg-Kohn variational principle is applied to the Kohn-Sham

orbitals, the canonical Kohn-Sham equations are obtained:

$$[-\frac{1}{2}(\partial^2/\partial\tau^2)_i + V_{\text{eff}}] \psi_i = \epsilon_i \psi_i$$

where τ includes coordinate x , y , and z and i runs over all electrons, ϵ_i is the Kohn-Sham eigenvalue of electron i , and the effective potential is:

$$V_{\text{eff}}(\mathbf{r}) = V_{\text{ext}}(\mathbf{r}) + \int d\mathbf{r}' \rho(\mathbf{r}')/|\mathbf{r}-\mathbf{r}'| + V_{\text{xc}}(\mathbf{r})$$

where $r^2 = x^2 + y^2 + z^2$. Here V_{ext} is the external potential, and the exchange-correlation potential is defined as the functional derivative of the exchange and correlation energy with respect to the density:

$$V_{\text{xc}}(\mathbf{r}) = \partial E_{\text{xc}}[\rho(\mathbf{r})]/\partial\rho(\mathbf{r})$$

These equations are nonlinear like the Hartree-Fock equations and are thus solved by an equivalent self consistent (iterative) procedure. The resulting density:

$$\rho(\mathbf{r}) = \sum_I \Psi_i^*(\mathbf{r}) \Psi_i(\mathbf{r})$$

and the Kohn-Sham eigenvalues then give the total ground state energy using either of two equivalent solutions:

$$E_{\text{tot}}(\rho) = T_s(\rho) + U(\rho) + H(\rho) + E_{\text{xc}}(\rho)$$

Or:

$$E_{\text{tot}}(\rho) = \sum_I (\epsilon_i) - \frac{1}{2} \int d\mathbf{r} d\mathbf{r}' \rho(\mathbf{r}) \rho(\mathbf{r}')/|\mathbf{r}-\mathbf{r}'| + E_{\text{xc}}(\rho) - \int d\mathbf{r} V_{\text{xc}}(\mathbf{r}) \rho(\mathbf{r})$$

The non-local extension to LDA is necessary because molecules are realistically in a heterogeneous electron gas, not a homogeneous one. A hybrid functional employs Hartree-Fock treatment for the exchange term as repulsion integrals. B3LYP is a particular density functional method due to Lee, Yang and Parr, and B3 signifies a 3 parameter functional due to Axel Becke.^{23a}

IIID) Semi-empirical methods

These methods follow directly from Hartree Fock models, and are based on the simplification that valence electrons are the only ones to be considered in the calculations. The inner electrons are regarded as a part of a fixed core. The central approximation in the semiempirical methods is to assume that atomic orbitals residing on different atoms do not overlap. The semi-empirical method relies on parameterization of atomic orbital interactions, and these adjustable parameters are chosen to reproduce equilibrium geometries, enthalpies of formation, ionization potentials and dipole moments. The AM1²⁷ and PM3²⁸ models use the same approximations for differential overlap, but differ in their parametrization. AM1 and PM3 are extensions to the MNDO method which signifies Modified Neglect of Diatomic Overlap. Diatomic overlap refers to interaction of atomic orbitals on different atomic centers.

The earlier AM1 is parametrized for H, C, N and O, the so called organic elements. PM3 stands for parametrized model 3 and it has the advantage over AM1 in that it is parametrized for more atoms (i.e., 3rd row nonmetals plus aluminum and halogens) than is AM1. It thus allows a wider range of molecules in the computations. AM1 and PM3 are parametrized to yield the energies of molecules in the form of

standard enthalpies of formation (where the enthalpies of the elements are set to zero at 298K and 1 bar). This stands in contrast to the Hartree-Fock model, which yields total energy E_{tot} at 0K (where the zero-energy state is a frozen nuclear framework and the separated electrons). AM1 was developed because the MNDO method failed to reproduce steric interference and hydrogen bonding. Energy effects were too positive for crowded molecules such as neopentane, and were too negative for molecules containing four-membered rings. Activation energies also tended to be too large. A common cause for the errors in MNDO is the tendency to overestimate repulsions between neighboring atoms. AM1 deals with this repulsion by adding additional gaussian functions, in the form of a core repulsion function (CRF), for any pair of atoms AB in the molecule.

$$\text{CRF}(AB) = z_A z_B \gamma_{ss} [1 + F(A) + F(B)]$$

$$\text{where } F(A) = \exp(-\alpha_A R_{AB}) + \sum_i K_{Ai} \exp[L_{Ai} (R_{AB} - M_{Ai})^2]$$

$$\text{and } F(B) = \exp(-\alpha_B R_{AB}) + \sum_j K_{Bj} \exp[L_{Bj} (R_{AB} - M_{Bj})^2]$$

where α , L , K and M are further adjustable parameters. Two ways were used to reduce the excessive interatomic repulsions at large separation. In the first, one or more attractive gaussians were added to compensate directly. In the second, repulsive gaussian functions were centered at smaller internuclear separations.

The MNDO method which is the basis for AM1 and PM3 methods is itself based on the Hartree-Fock method. The treatment with MNDO is confined to the valence electrons of closed shell molecules. These electrons are assumed to move in the field of

the fixed core potentials of the nuclei and of the inner shell electrons (core repulsion).

The valence shell MO's, Ψ_i are represented by linear combination of a minimum basis set of valence shell AO's, Φ_v :

$$\Psi_i = \sum_v C_{vi} \Phi_v$$

The coefficients C_{vi} are found from the Roothan-Hall equations (the variation method) which assume the form :

$$\sum_v (F_{\mu\nu} - E_i \delta_{\mu\nu}) = 0$$

where E_i is the eigenvalue of the MO Ψ_i and $\delta_{\mu\nu}$ is the Kronecker δ . The elements $F_{\mu\nu}$ of the Fock matrix are the sum of a one electron part $H_{\mu\nu}$ (core Hamiltonian), and a two-electron part $G_{\mu\nu}$;

$$F_{\mu\nu} = H_{\mu\nu} + G_{\mu\nu}$$

and then the electronic energy E_{el} is given by;

$$E_{el} = \frac{1}{2} \sum_{\mu} \sum_{\nu} P_{\mu\nu} (H_{\mu\nu} + F_{\mu\nu})$$

where $P_{\mu\nu}$ is an element of the bond order matrix.

It is assumed that AO's Φ_{μ} and Φ_{ν} are centered at atom A and the AO's Φ_{λ} and Φ_{σ} are at atom B ($A \neq B$). The Fock matrix elements then are :

$$F_{\mu\mu} = U_{\mu\mu} + \sum_B V_{\mu\mu, B} + \sum_{\nu, A} P_{\nu\nu} [(\mu\mu, \nu\nu) - \frac{1}{2} (\mu\nu, \mu\nu)] + \sum_B \sum_{\lambda, \sigma} P_{\lambda\sigma} (\mu\mu, \lambda\sigma)$$

$$F_{\mu\nu} = \sum_B V_{\mu\nu, B} + \frac{1}{2} P_{\mu\nu} [3(\mu\nu, \mu\nu) - (\mu\mu, \nu\nu)] + \sum_B \sum_{\lambda, \sigma} (\mu\nu, \lambda\sigma)$$

$$F_{\mu\lambda} = \beta_{\mu\lambda} - \frac{1}{2} \sum_{\nu, A} \sum_{\sigma, B} P_{\nu\sigma} (\mu\nu, \lambda\sigma)$$

The Fock matrix has the following six terms:

- 1) One-center one-electron energies $U_{\mu\nu}$ which represent the sum of the kinetic energy of an electron in AO Φ_μ at atom A and its potential energy due to the attraction of the core of atom A. $U_{\mu\nu}$ assumes the following form:

$$U_{\mu\nu} = (\partial^2 \Phi_\mu / \partial \tau_1) - (e^2 / r_1) \Phi_\mu d\tau$$

- 2) One-center two-electron repulsion integrals, i.e., Coulomb integrals.

$$(\mu\mu, \nu\nu) = g_{\mu\nu}$$

- 3) Exchange integrals

$$(\mu\nu, \mu\nu) = h_{\mu\nu}$$

- 4) Two-center one-electron core resonance integrals $\beta_{\mu\lambda}$ which have the following form:

$$\beta_{\mu\lambda} = \int \Phi_\mu (e^2 / r_B) \Phi_\lambda d\tau_\lambda$$

- 5) Two center one electron attractions $V_{\mu\nu, B}$ between an electron in the distribution

$\Psi_\mu \Psi_\nu$ at atom A and the core of atom B.

- 6) Two-center two-electron repulsion integrals $(\mu\nu, \lambda\sigma)$. These integrals represent the energy of interaction between the charge distribution at atom A and atom B, and they have the following form:

$$(\mu\nu, \lambda\sigma) = \iint \Phi_\mu^{*(1)} \Phi_\nu^{(1)} [1/r_{12}] \Phi_\lambda^{*(2)} \Phi_\sigma^{(2)} d\tau_1 d\tau_2$$

The total energy of the molecule E_{tot} is the sum of the electronic energy E_{el} and the repulsions between the cores of atoms A and B ($E_{\text{AB}}^{\text{core}}$).

$$E_{\text{tot}}^{\text{mol}} = E_{\text{el}} + \sum_A \sum_B E_{\text{AB}}^{\text{core}}$$

The heat of formation of the molecule is obtained from its total energy by subtracting the electronic energies and adding the experimental heats of formation of the atoms in the molecule:

$$\Delta H_f^{\text{mol}} = E_{\text{tot}}^{\text{mol}} - \sum_A E_{\text{el}}^{\text{A}} + \sum_A \Delta H_f^{\text{A}}$$

The electronic energies of the atoms are calculated from restricted single-determinantal wave functions using the same approximations and parameters as in molecular NDDO calculations.

III E) Definition and meaning of the standard deviation.

The standard deviation of the slope of a line is defined as the best fit (minimized deviations of all points) of a slope of a line determined by a set of measurements (X_i, Y_i) . This slope is determined by choosing the value which minimizes the sum of the squares of the deviations of these measurements. For a set of measurements X_i the most probable value of X is that which minimizes the quantity $\sum (X - X_i)^2$, where X can be varied to obtain the minimum value of the sum.

If two variables X and Y are related linearly by the following equation:

$Y = mX + b$, where m is the slope of the line and b is the intercept with Y axis and if a series of N measurements $(X, Y)_i$ is made in which the error is in Y_i only, then the

normal equations are: $m \sum X_i + bN = \sum Y_i$ and $m \sum X_i^2 + b \sum X_i = \sum X_i Y_i$ and the most probable value of the slope is given by:

$$m = \frac{N \sum X_i Y_i - (\sum X_i)(\sum Y_i)}{N \sum X_i^2 - (\sum X_i)^2}$$

The errors in m and b are produced by errors in the Y_i values which are taken all from the parent distribution with variance σ^2 . The variance in the slope of the line m is given by the following equation: $\sigma_m^2 = N\sigma^2/\Delta$

$$\text{where } \Delta = N \sum X_i^2 - (\sum X_i)^2 \text{ (Dispersion)}$$

N is the number of measurements and σ^2 is the variance in the parent distribution and σ_m^2 is the variance in the slope of the line. The standard deviation in the slope m of the line is σ_m .

IIIF) Choice of Substituent parameters.

There are various measurements of substituent electronic effects proposing to account for inductive (along σ bonds) and resonance (along π bonds) electron withdrawing and donating tendencies. Often these depend upon the nature of the accepting substrate. We chose a standard classical set of Hammett σ_p and σ_m parameters most familiar to practicing organic chemists, and noted that σ_m reflects predominantly inductive effects while σ_p includes mainly resonance effects.

IV) Results and discussion

IVA) Correlation between experimental and computational data.

The computational method that correlated best with experimental data was the semiempirical method at PM3 and AM1 levels. Table 1 shows values for experimental and calculated enthalpies for different dienes and dienophiles in the Diels-Alder reaction.

Table 1: Experimental and calculated values of reaction enthalpy of Diels-Alder reactions using semiempirical, density functional and Hartree-Fock methods.

Method	Reaction (Table 2)	Reaction enthalpy (computed) (kcal/mol)	Reaction enthalpy (experimental) ^a (kcal/mol)
PM3	1	-52.5	-36.3
AM1		-56.4	
HF 6-311G*		5.42	
pBPDN**		4.76	
PM3	2	-19.3	-17+/- 1
AM1		-22.7	
pBPDN**		4.5	
PM3	3	-22	-19.3+/- 1.9
AM1		-23	
HF 6-311G*		4.55	
PBPDN**		4.1	
PM3	4	-14.69	-13.95
AM1		-12.2	
HF 6-311G*		-15.63	
PBPDN**		-14.85	
PM3	5	-37.9	-43.8+/- 2.8
AM1		-39.2	
HF 6-311G*		-15.13	
PBPDN**		-13.98	
PM3	6	25.3	26.3
AM1		29.3	
HF STO-3G		-21.74	
HF 321G*		-20.9	
PBPDN**		-18.69	

a) experimental values are given in Table 2.

Table 1 shows only in one case (Reaction 5) is AM1 closer than PM3 to the experimental values, and PM3 is closest in the other five reactions (Table 2). This is reasonable since AM1 is parametrized only for H, C, N, and O while PM3 is parametrized for additional third row elements. (Hartree-Fock and the pBPDN** Density Functional methods were also found inadequate.) Therefore we chose to make most of our calculations using the PM3 model of approximation.

Table 2: Types of Diels-Alder reactions.

1) Ethylene and butadiene cycloaddition. ³¹
2) Dimerization of cyclopentadiene. ¹²
3) Cycloaddition reaction of cyclopentadiene and acrolein. ¹²
4) Cycloaddition reaction of 2-methyl furan and maleic anhydride. ²⁵
5) Cycloaddition reaction of tetracyanoethylene and isoprene. ³²
6) Cycloaddition reaction of 2-methoxy furan and dimethylacetylene dicarboxylate. ²⁹

IVB) Effect of substituent on the energy levels of the HOMO and LUMO of the diene.

Substituting the heterocyclic ring on the 3 and 4 positions with electron donating groups has the effect of destabilizing the HOMO and LUMO of the ring, while substituting the ring with electron withdrawing groups has the effect of stabilizing the energy levels of the HOMO and LUMO of the ring as is shown in table 3. This effect is similar to that observed with normal dienes used in the Diels-Alder reaction such as butadiene. In general one might anticipate the closer (HOMO) tends to be somewhat more sensitive to substituents inductive or resonance effects than the more remote (LUMO) levels. This frequently occurs in atomic spectroscopy when nuclear charge is changed and one observes the diminishing effect on more outlying orbitals

Table 3: Calculated E_{HOMO} and E_{LUMO} Values for 3,4 disubstituted pyrrole, furan, thiophene and phosphole using AM1 and PM3

Compound	E_{HOMO} (ev)(AM1)	E_{LUMO} (ev)AM1	E_{HOMO} (ev)PM3	E_{LUMO} (ev)PM3
Pyrrole	-8.656	1.378	-8.93	1.114
Pyrrole 3,4 diformic acid dimethylester	-9.748	0.104	-9.89	-0.0379
3,4 dimethoxy pyrrole.	-8.56	1.14	-8.054	1.01
Pyrrole 3,4 bis dimethyl amine	-8.17	1.328	-8.249	0.968
2,3 dicyanopyrrole	-9.72	-0.0276	-9.994	-0.251
Thiophene	-9.218	0.238	-9.54	-0.191
Thiophene 3,4 diformic acid dimethyl ester	-10.2	-0.84	-10.36	-1.33
3,4 dimethoxythiophene	-8.555	0.121	-8.91	-0.224
Thiophene 3,4 bis dimethyl amine	-8.204	0.315	-8.74	-0.153
3,4 dicyanothiophene	-10.043	-0.96	-10.3	-1.436
Furan	-9.317	0.723	-9.376	0.609
Furan 3,4 diformic acid dimethyl ester	-10.34	-0.565	-10.296	-0.531
Furan 3,4 bis-dimethyl amine	-8.6	0.779	-8.64	0.572
3,4 dicyanofuran	-10.308	-0.624	-10.36	-0.789
3,4 dimethoxyfuran	-9.125	0.552	-9.01	0.541
Phosphole	-9.4	-0.025	-8.8	-0.041
Phosphole 3,4 bis-dimethyl amine	-8.34	0.15	-9.33	-0.034
Phosphole 3,4 diformic acid dimethyl ester	-10.202	-1.166	-8.41	-0.825
3,4-dicyano-phosphole	-10.24	-1.48	-10.1	-1.2
3,4-dimethoxy-phosphole	-8.9	0.34	-8.1	0.24

IVC) Correlation between E_{HOMO} and E_{LUMO} with σ_p and σ_m

The energy levels of the HOMO and the LUMO of the four heterocyclic compounds correlated linearly with σ_p and σ_m . Positive values of σ refer to electron withdrawing groups while negative values refer to electron donating groups. The values of σ indicate the net substituent effect in electron donating or electron withdrawing inductively along σ bonds or mesomerically along π bonds. Figures 1 to 14 show the correlation between E_{HOMO} and E_{LUMO} with σ_p and σ_m for the four heterocyclic compounds.

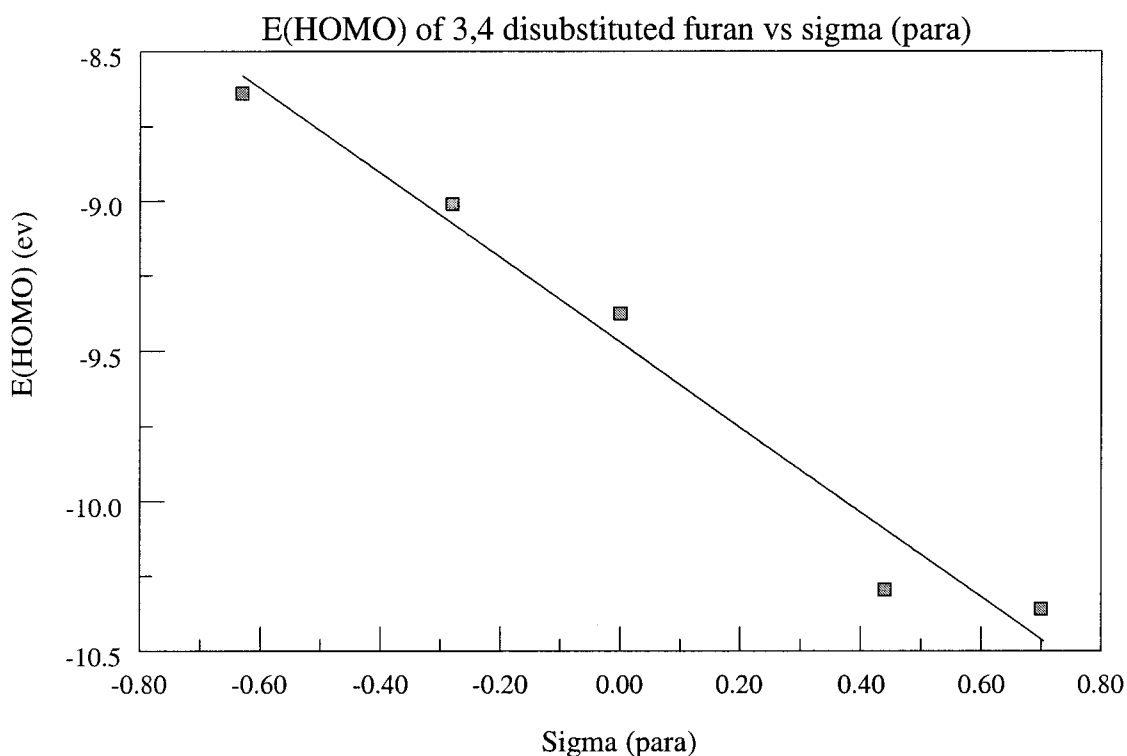


Figure 1: Plot of $E(\text{HOMO})$ of the designated furan system.

The absolute error in the calculations is difficult to estimate a priori so that the point size is arbitrary. The “standard deviation” is strictly a statistical quantity applicable to all graph points.

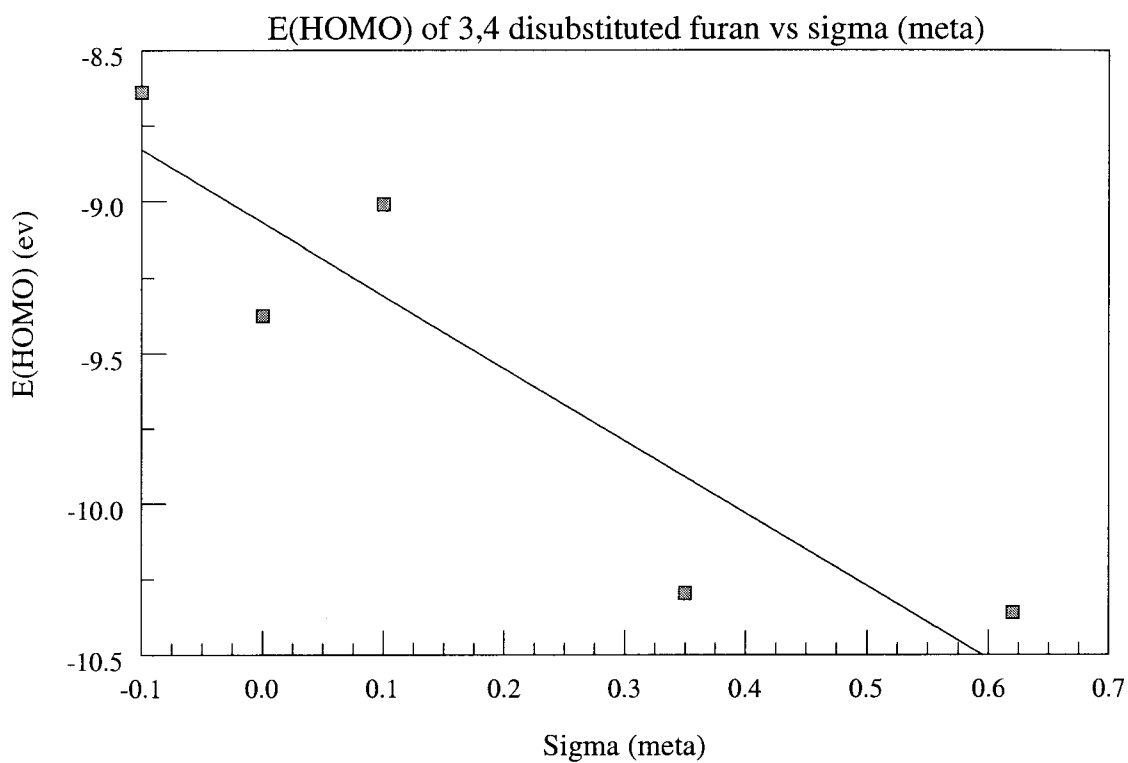


Figure 2: Plot of E(HOMO) of the designated furan system.

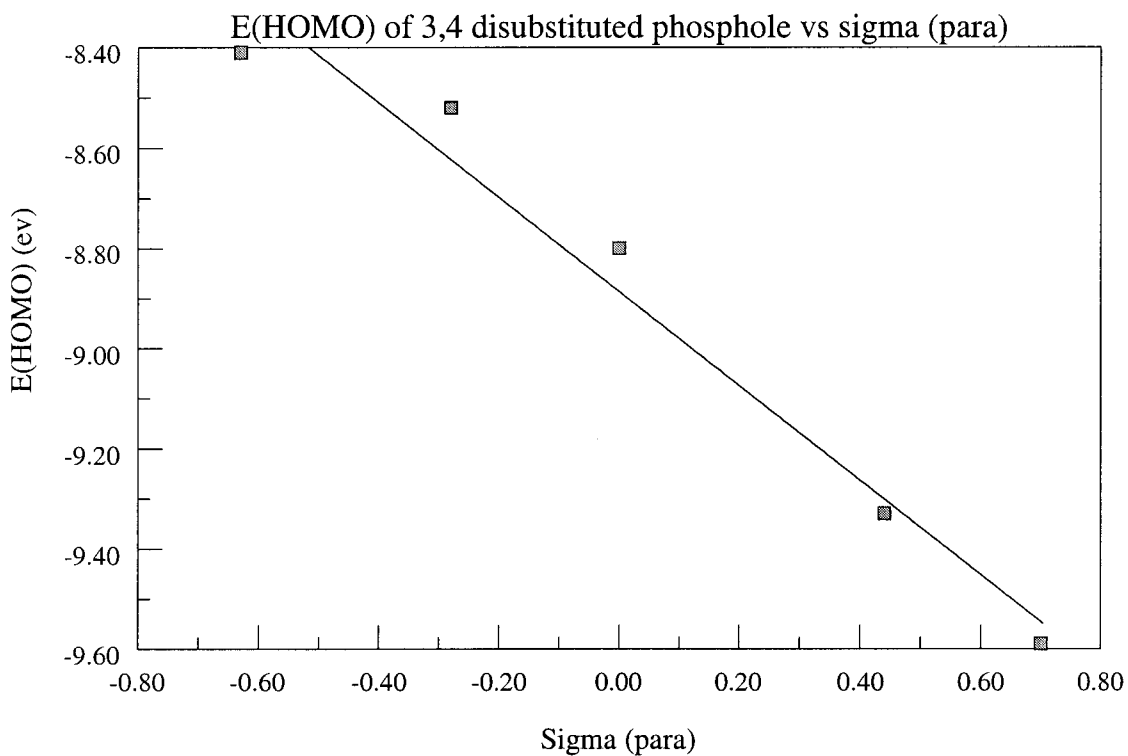


Figure 3: Plot of E(HOMO) of titled phosphole system .

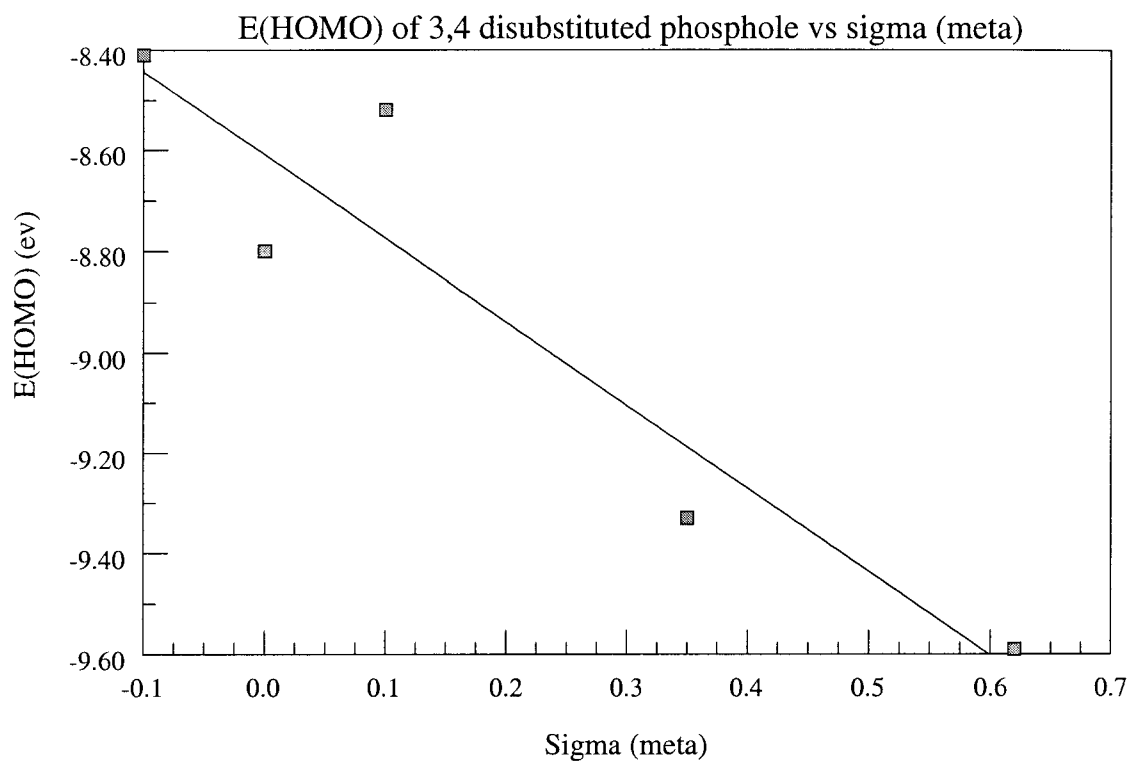


Figure 4: Plot of E(HOMO) of the noted phosphole system.

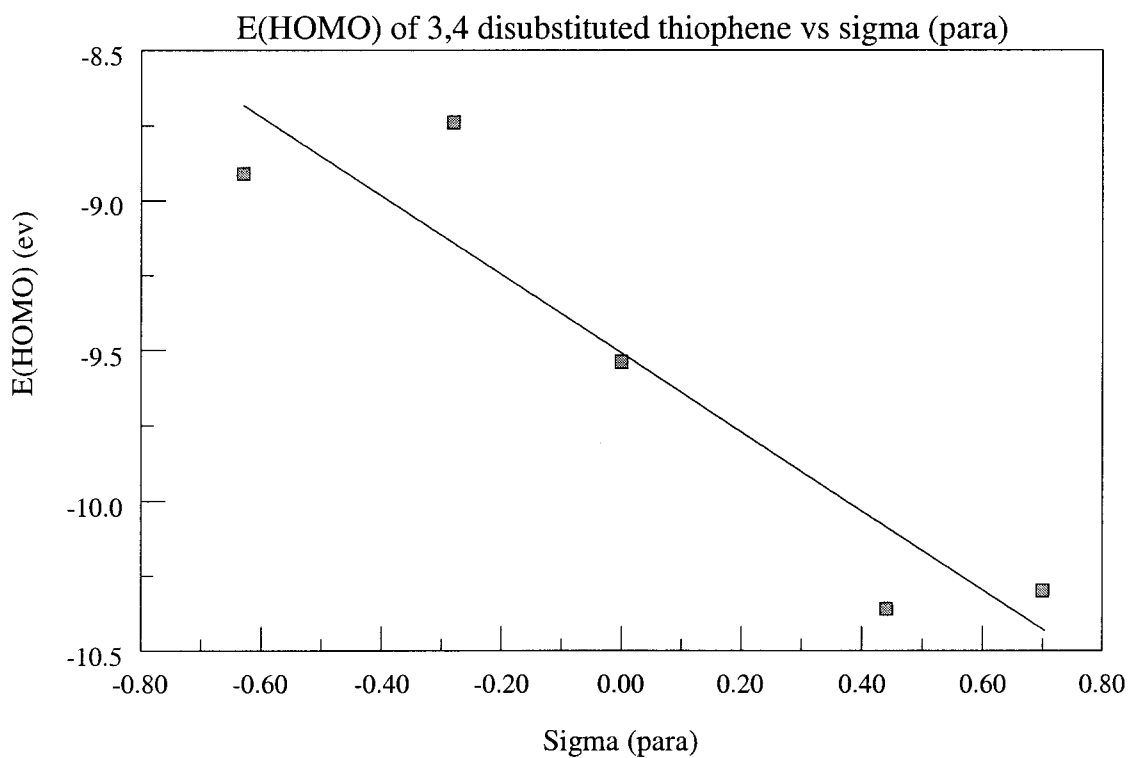


Figure 5: Plot of E(HOMO) of the designated thiophene system.

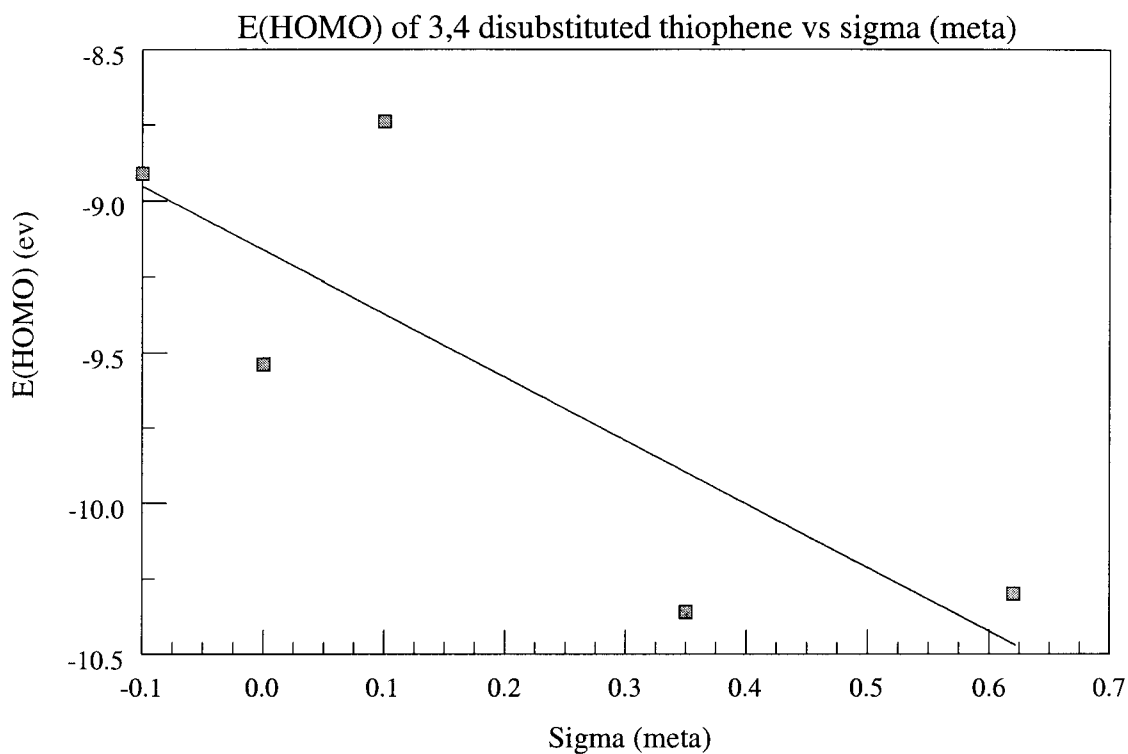


Figure 6: Plot of E(HOMO) of the noted thiophene system.

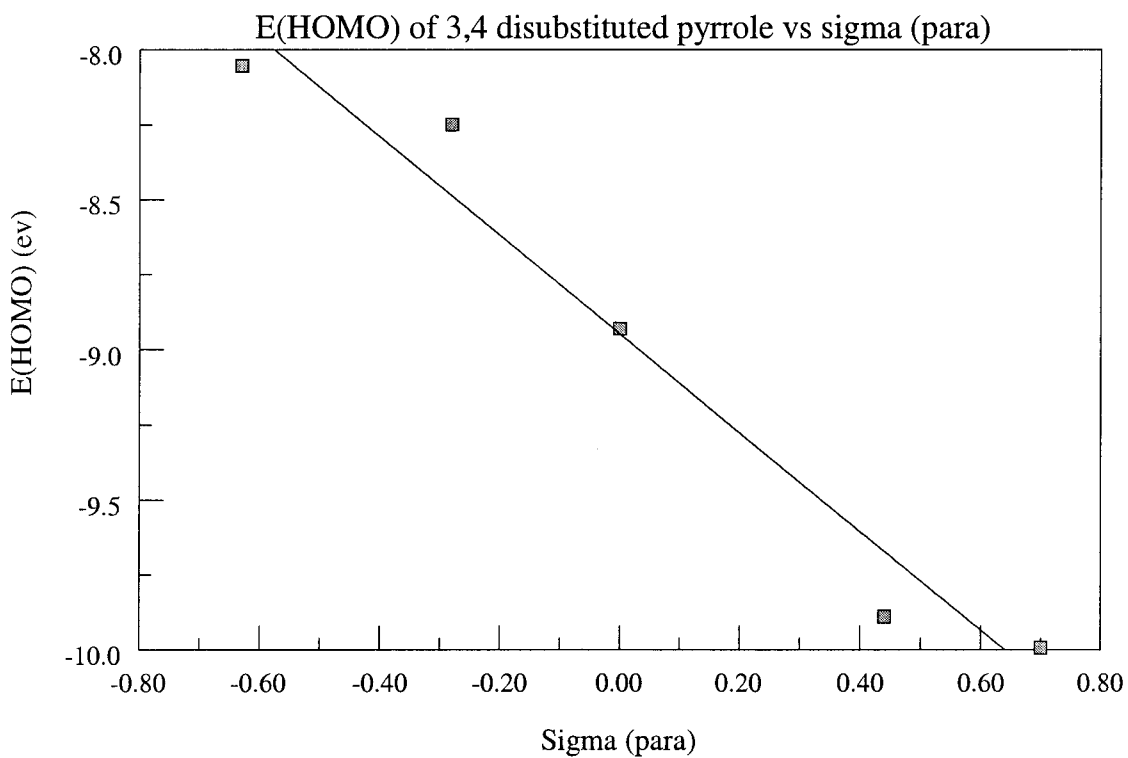


Figure 7: Plot of E(HOMO) of the designated pyrrole system.

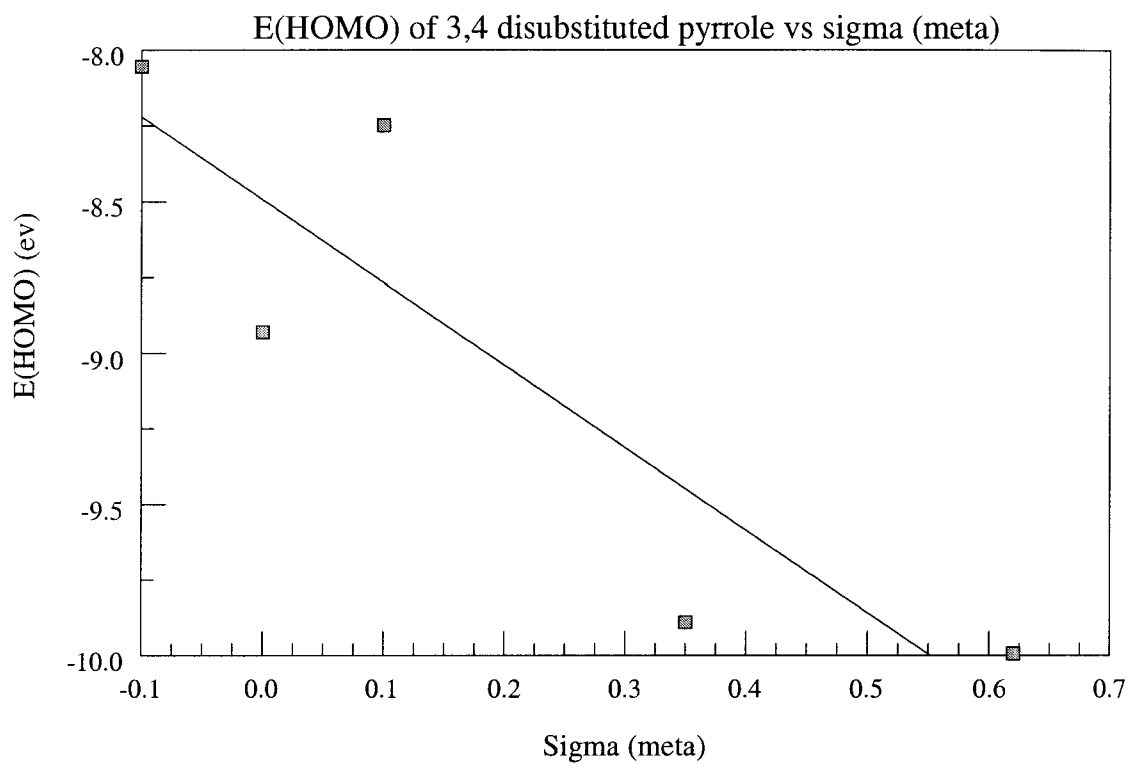


Figure 8: Plot of E(HOMO) of the titled pyrrole system.

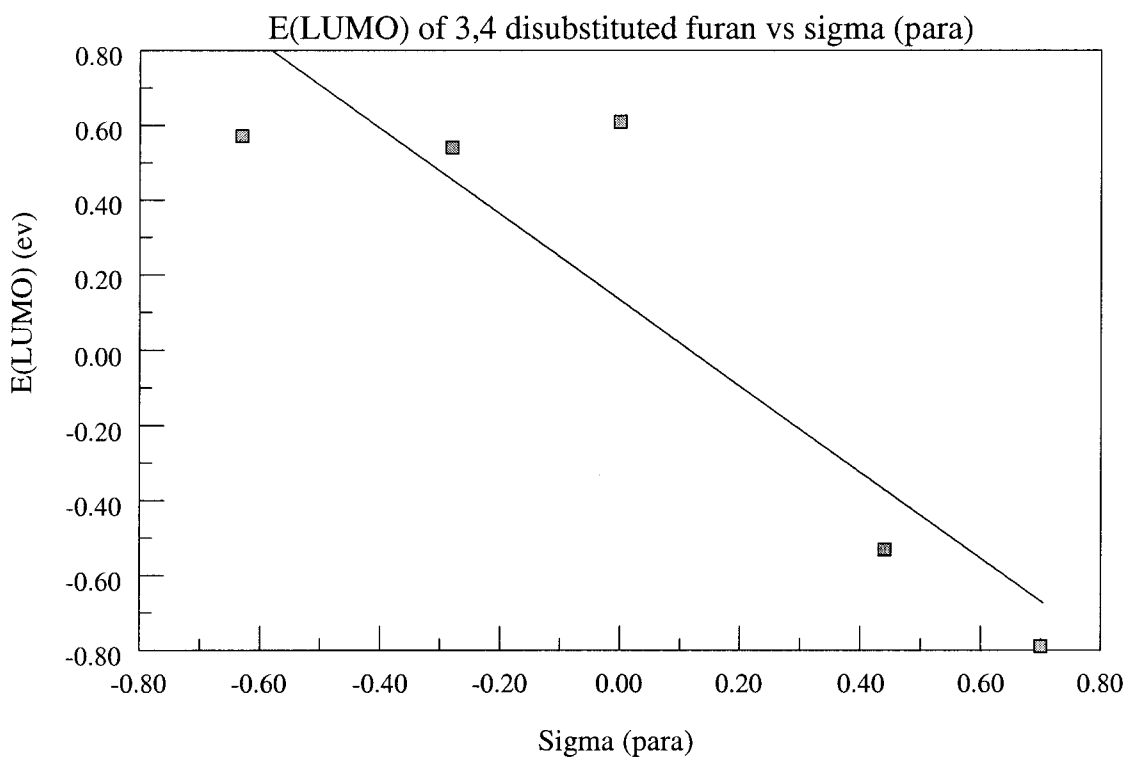


Figure 9: Plot of E(LUMO) of the titled furan system.

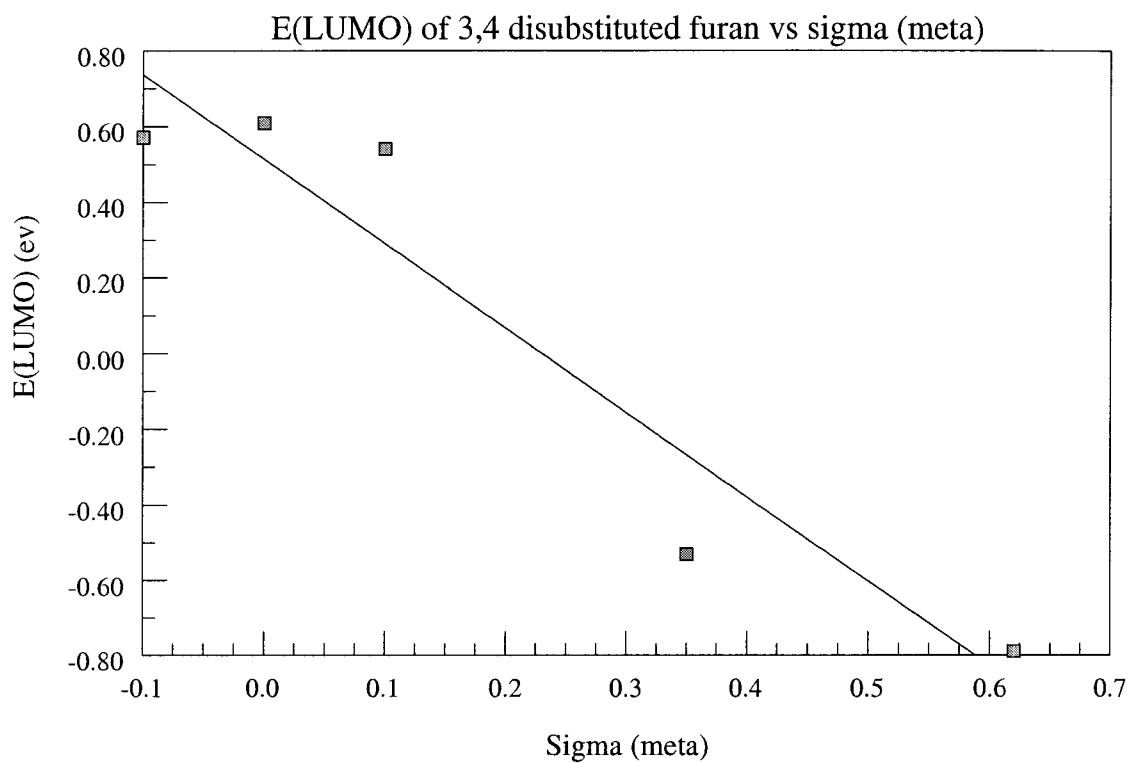


Figure 10: Plot of E(LUMO) of the referenced furan system.

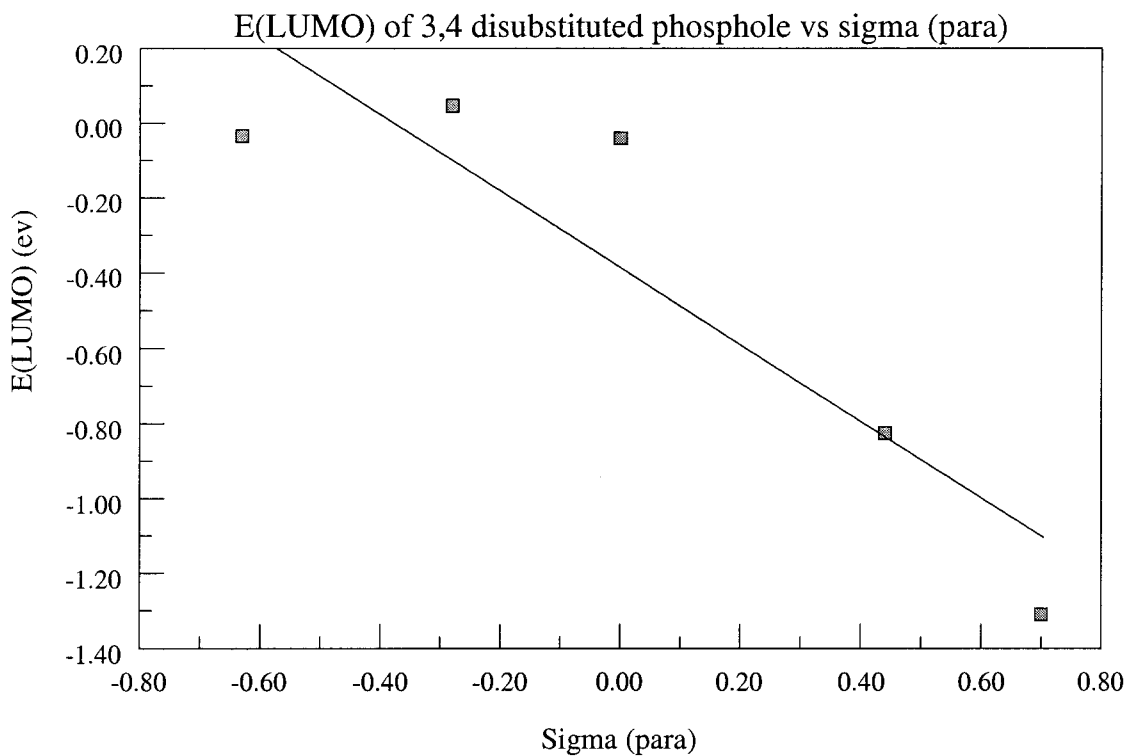


Figure 11: Plot of E(LUMO) of the captioned phosphole system.

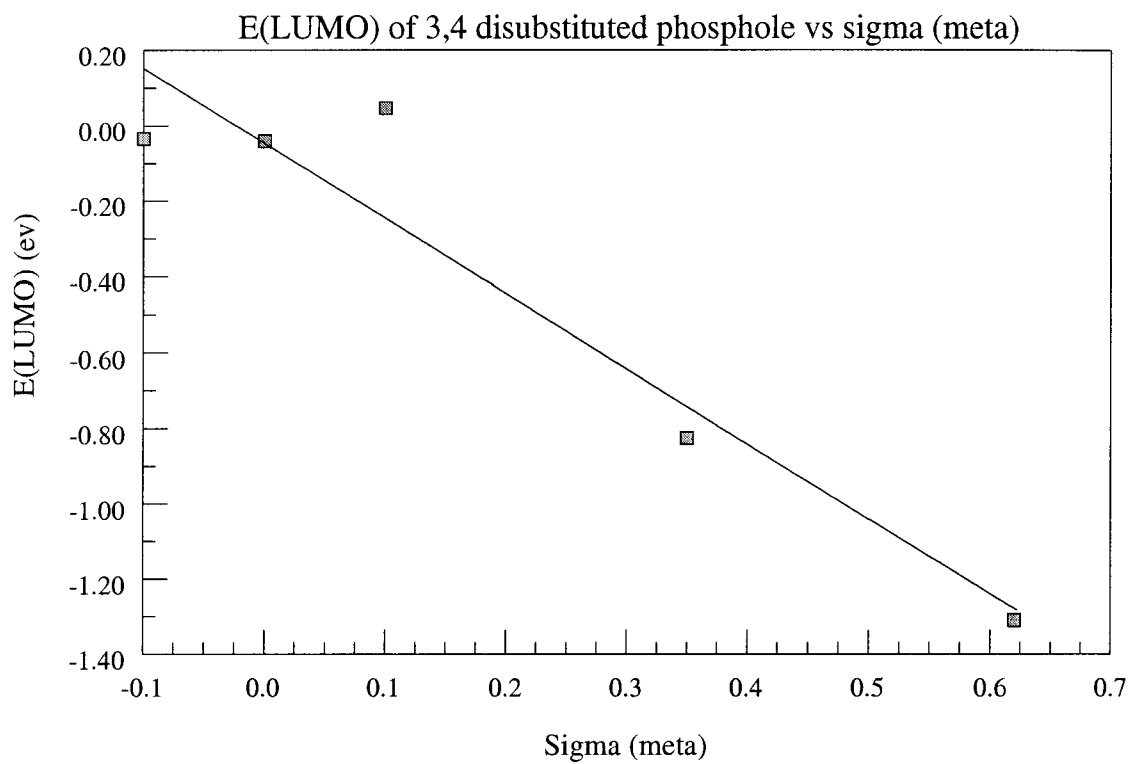


Figure 12: Plot of E(LUMO) of the titled phosphole system.

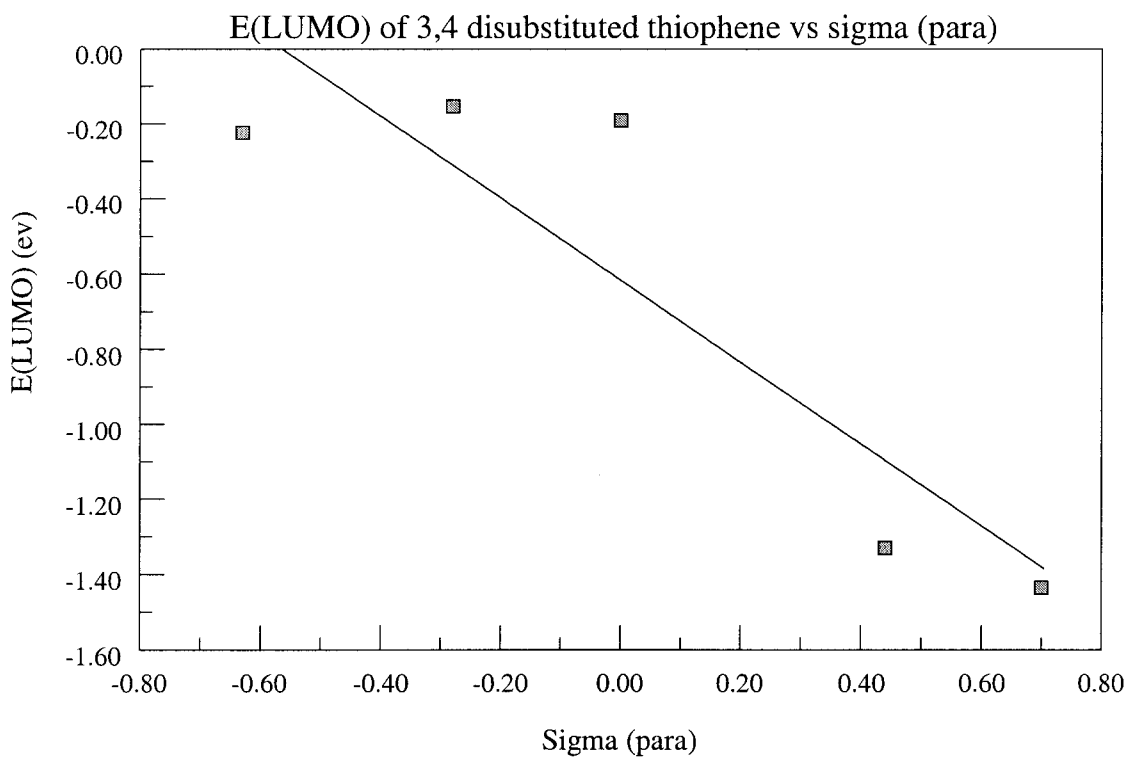


Figure 13: Plot of E(LUMO) of the referenced thiophene system.

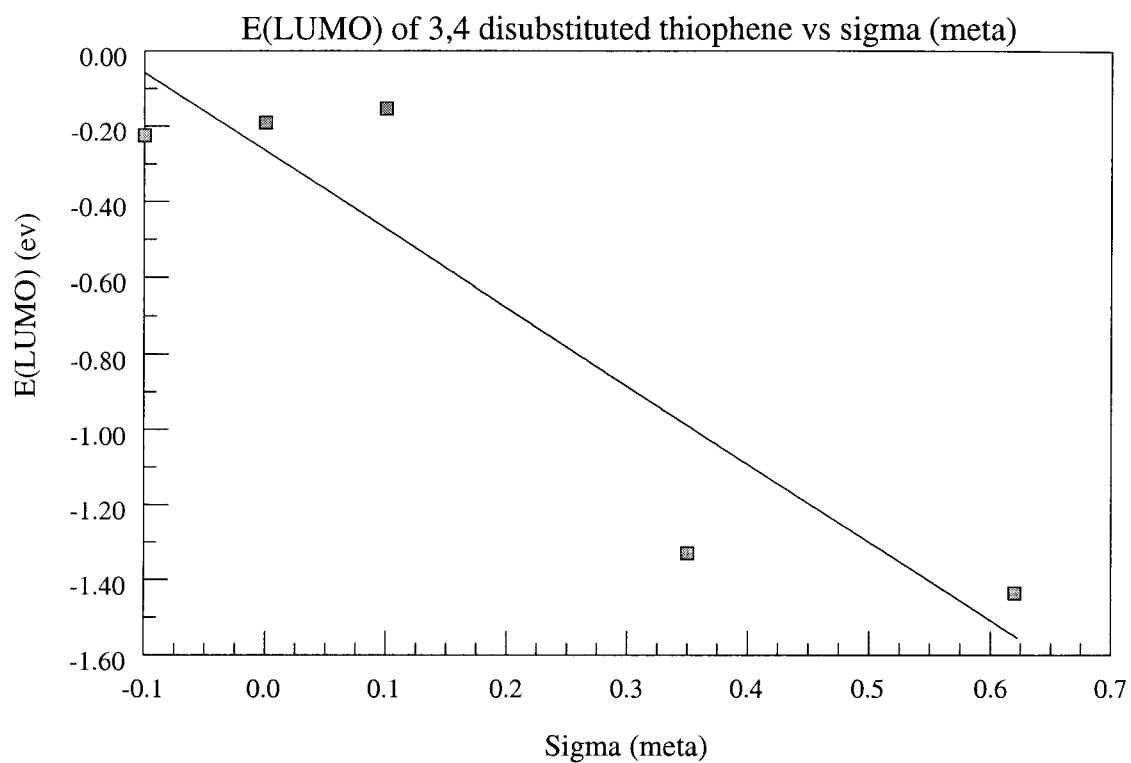


Figure 14: Plot of E(LUMO) of the referenced thiophene system.

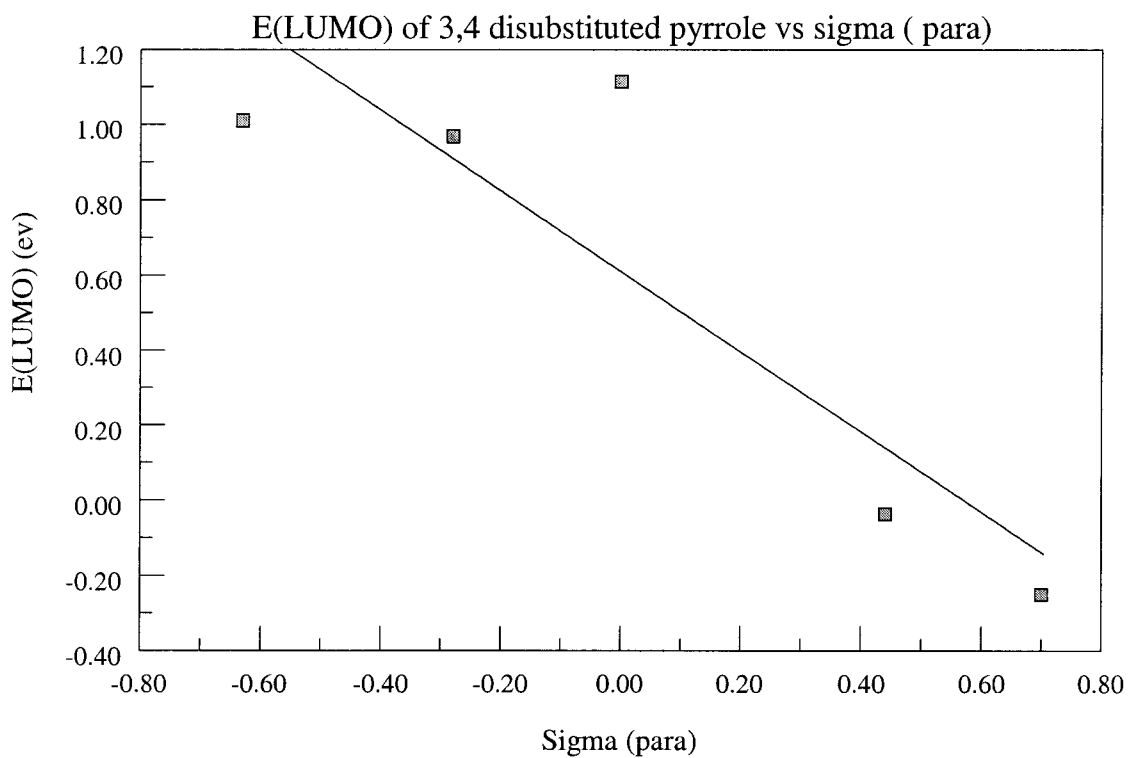


Figure 15: Plot of E(LUMO) of the captioned pyrrole system.

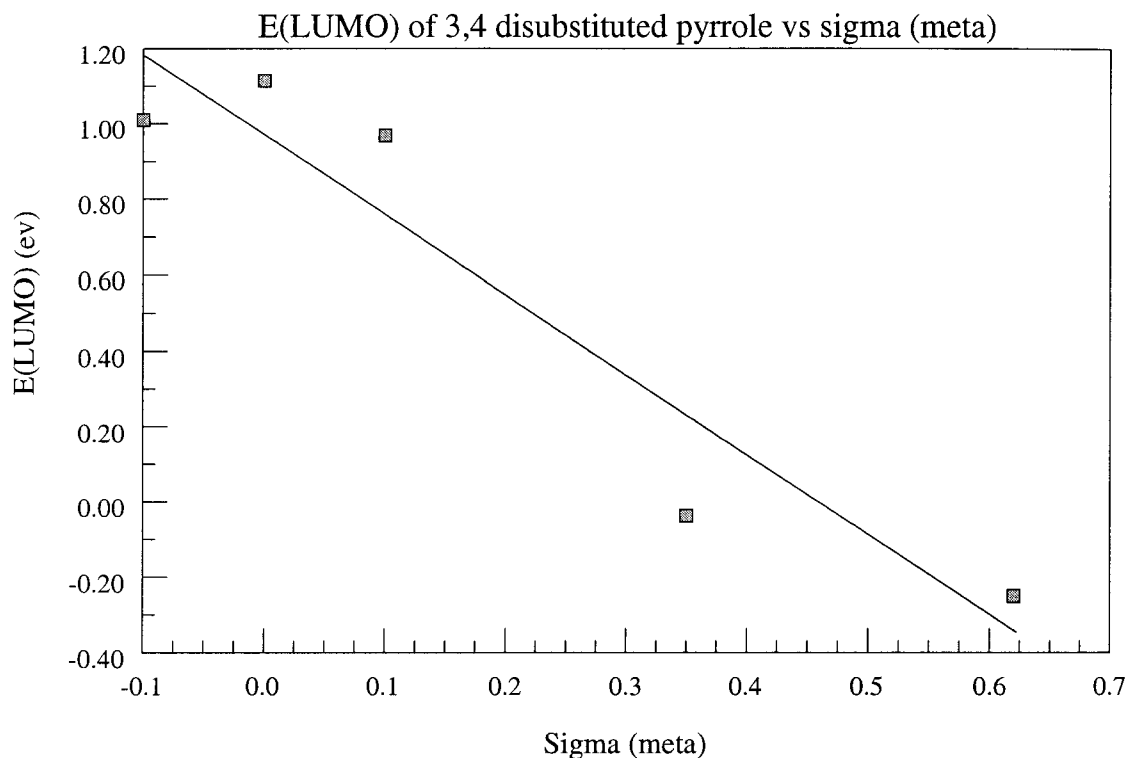


Figure 16: Plot of E(LUMO) of the titled pyrrole system.

Table 4: Least square summary of the plots of E_{HOMO} and E_{LUMO} of the dienes vs σ_{p} and σ_{m} of diene substituents.

System	Slope and standard deviation of the lines	Figure
E_{HOMO} of furan vs σ_{p}	-1.4+/- 0.2	1
E_{LUMO} of furan vs σ_{p}	-1.1+/- 0.3	9
E_{HOMO} of furan vs σ_{m}	-2.4+/- 0.4	2
E_{LUMO} of furan vs σ_{m}	-2+/- 0.2	10
E_{HOMO} of pyrrole vs σ_{p}	-1.6+/- 0.2	7
E_{LUMO} of pyrrole vs σ_{p}	-1+/- 0.4	15
E_{HOMO} of pyrrole vs σ_{m}	-2.7+/- 0.5	8
E_{LUMO} of pyrrole vs σ_{m}	-2+/- 0.2	16
E_{HOMO} of thiophene vs σ_{p}	-1.3+/- 0.3	5
E_{LUMO} of thiophene vs σ_{p}	-1+/- 0.3	13
E_{HOMO} of thiophene vs σ_{m}	-2.1+/- 0.5	6
E_{LUMO} of thiophene vs σ_{m}	-2+/- 0.3	14
E_{HOMO} of phosphole vs σ_{p}	-0.94+/- 0.1	3
E_{LUMO} of phosphole vs σ_{p}	-1+/- 0.3	11
E_{HOMO} of phosphole vs σ_{m}	-1.7+/- 0.2	4
E_{LUMO} of phosphole vs σ_{m}	-2+/- 0.2	12

Since the standard deviations of the slopes of the correlations over all four dienes and five substituents averages to +/- 19% of the slope values themselves, a definite positive relationship between the variables is clearly indicated.

As anticipated earlier based on atomic spectroscopy results, the substituent effect on the closer HOMO orbitals is greater than on the more remote LUMO orbitals, averaged over these 20 compounds (average slope -1.77 for the HOMOs vs -1.51 for the LUMOs). However, the difference between these two quantities is nearly the same as the average standard deviations in either one (+/- 0.3 HOMO, or +/- 0.28 LUMO), so that the difference is suggestive rather than conclusive.

IVD) Correlation between log of equilibrium constant and σ_p and σ_m of Hammett.

Plotting the log of the equilibrium constant for the Diels-Alder reaction as a function of σ_p and σ_m gave a linear correlation between them as shown in figures 19 to 26. Table 5 shows least square summary of the plots of log Ke of the reactions of 3,4 disubstituted cyclic 5-membered aromatic rings with acrolein vs σ_p and σ_m of diene substituent. Table 5 shows values of the slopes and standard deviations for plots of log of equilibrium constant vs σ_p and σ_m of diene substituents. The table shows that the equilibrium constant is sensitive to the nature of the substituent on the diene. The more electron donating the substituent is the larger the equilibrium constant. Significantly a correlation is not evident with phosphole, because the value of the standard deviation exceeds that of the slope itself. This is probably related to the unique (among the 4 heterocycles) nonplanarity of the phosphole ring system, rendering it non-aromatic and thus less influenced by the σ_p or σ_m parameters.

Table 5- Least Square Summary of log Ke vs σ_p and σ_m of diene substituents

System	Slope and standard deviation of the lines	Figure
Log Ke vs σ_p of substituted furan with acrolein.	-2.3+/-2.0	23
Log Ke vs σ_m of substituted thiophene and acrolein.	-2.0 +/- 0.5	19
Log Ke vs σ_p of substituted pyrrole and acrolein.	-4.0+/-1.0	21
Log Ke vs σ_p of substituted phosphole with acrolein.	-0.4 +/- 0.5	17
Log Ke vs σ_m of substituted phosphole with acrolein.	-0.3 +/- 0.6	18

It is noteworthy that despite the exothermicities for these reactions (two pi bonds are essentially replaced by two sigma bonds), this favorable thermodynamic driving force is usually completely negated by the larger negative entropy effect due to the creation of a more complex bicyclic adduct from two simpler fragments. Table 6 presents the equilibrium constants for the four heterocyclic systems and shows the detailed substituent effect for each. Only the phosphole group of molecules and the methoxy-furans show equilibrium constants larger than 10, suggesting the difficulty of successful synthesis of most of the other [2.2.1] bicyclic compounds by the Diels-Alder condensation. Despite such thermodynamic prohibitions, however, furan⁴, pyrrole⁵ and alkyl substituted phosphole⁶ have been successfully derivatized into Diels-Alder adducts with appropriate dienophiles. For these systems PM3 also predicts favorable ($\Delta G^0 < 0$) equilibrium constants at 25°C as should be expected. However, for the normally unreactive

thiophenes very small equilibrium constants are calculated, again reflecting the observed low level of reactivity.

Table 6: Log K_e values of endo reaction between 3,4 disubstituted furan, thiophene, pyrrole and phosphole with acrolein as a function of substituent on the diene.

-CN	-C(O)OCH₃	-H	CH₃O-	(CH₃)₂N-	System
2.64	2.99	3.60	2.80	3.5	Phosphole
-10.0	-9.55	-6.83	-4.65	-5.64	Pyrrole
-2.53	-4.59	-3.00	1.45	-1.60	Furan
-9.92	-9.83	-8.52	-7.26	-7.78	Thiophene

In general we note also that there is a lack of correlation for $\log K_e$ vs σ_m or σ_p for phosphole and furan derivatives, while there is a reasonable correlation for thiophene and pyrrole. This is perhaps due to the lack of planarity of the phosphole ring and the zero value for the p-orbital coefficient on the O-atom in furan. These features reduce the aromaticity and likewise the sensitivity to the substituents resonance component. In the case of thiophene and pyrrole these two circumstances are not present, and thus they are more aromatic so that the substituent effect is more evident.

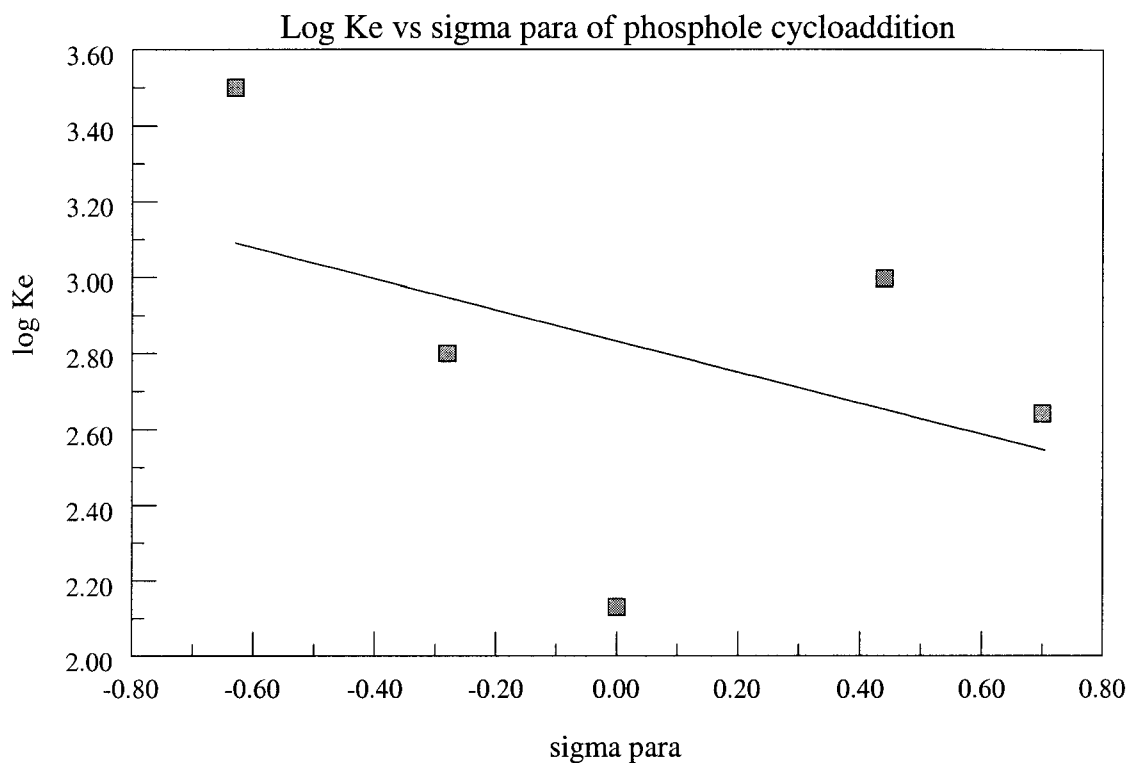


Figure 17: Plot of log Ke of the titled phosphole system.

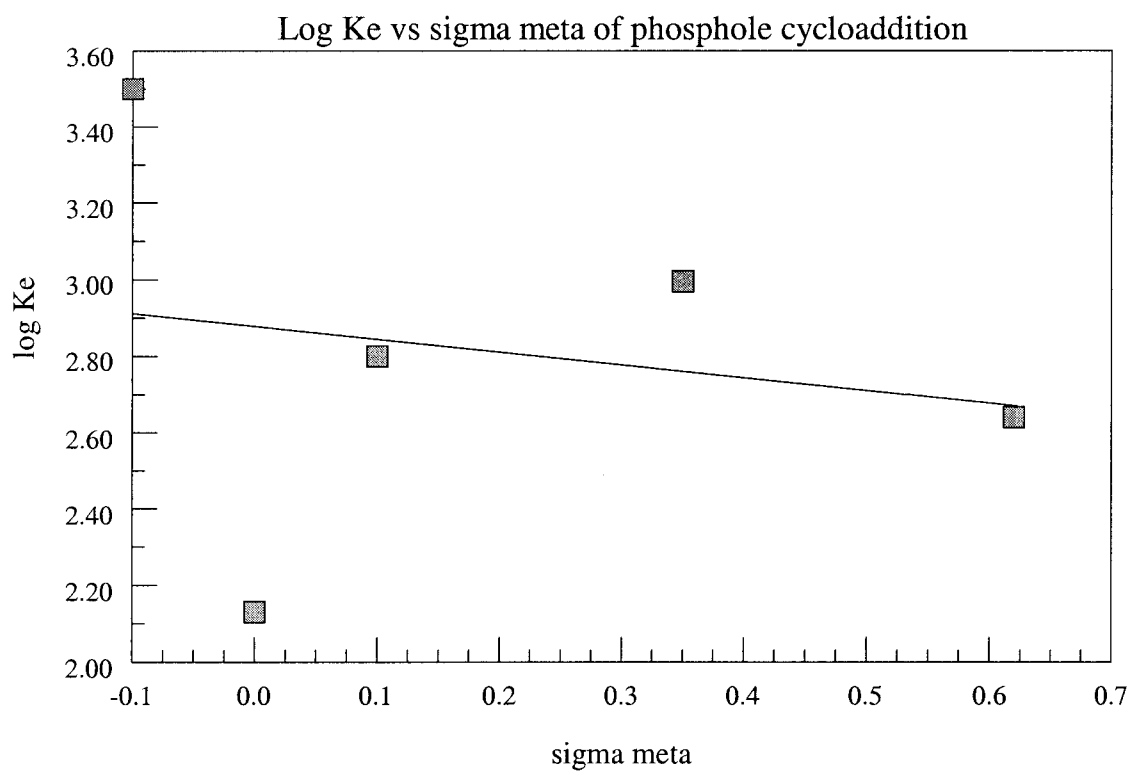


Figure 18: Plot of log Ke of the referenced phosphole system.

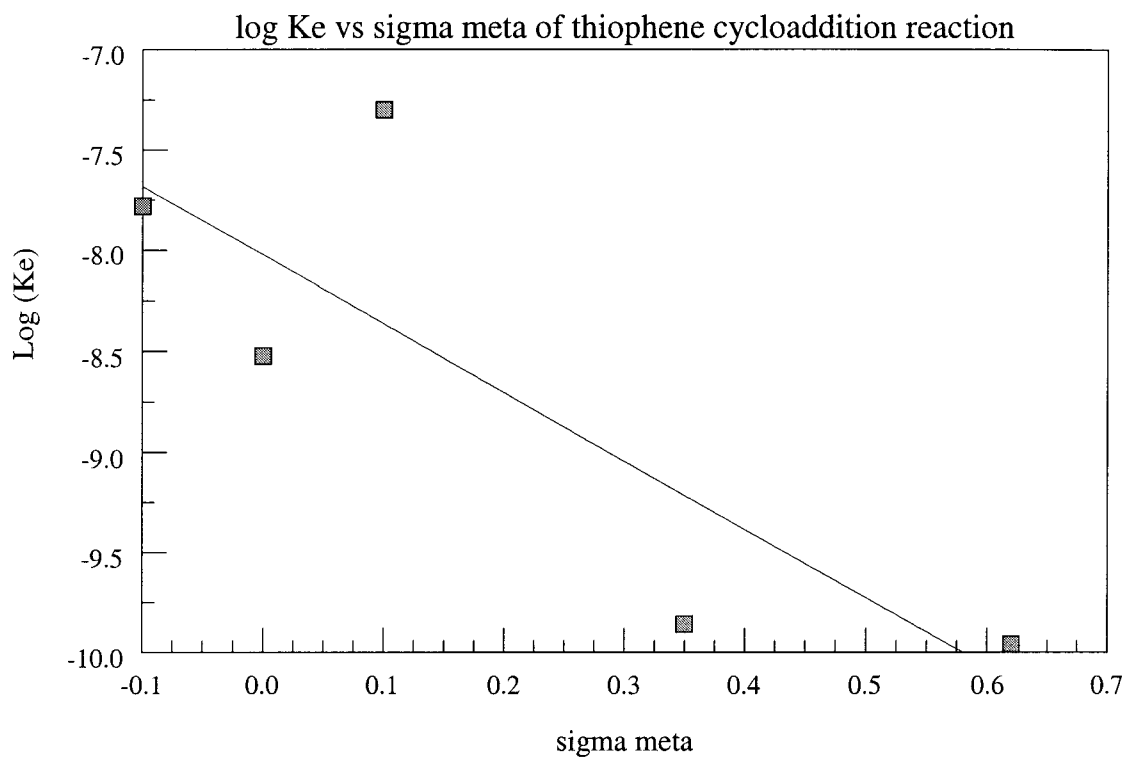


Figure 19: Plot of log Ke of the titled thiophene system.

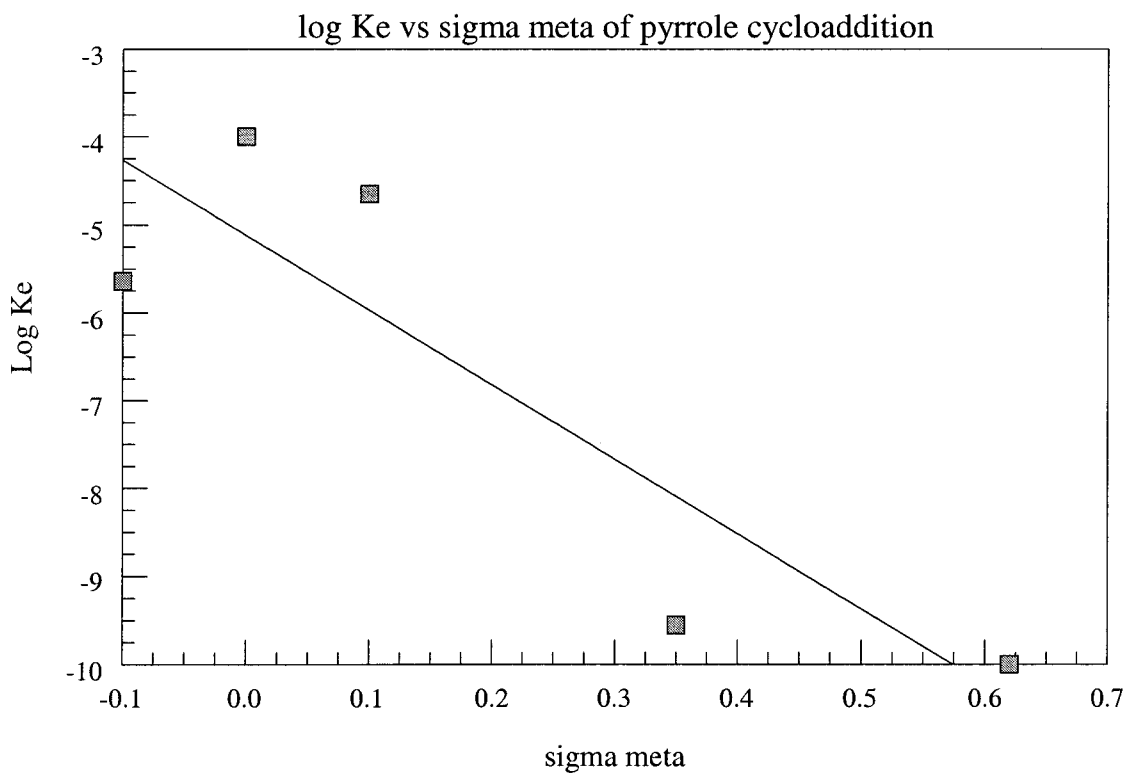


Figure 20: Plot of log Ke of the referenced pyrrole system.

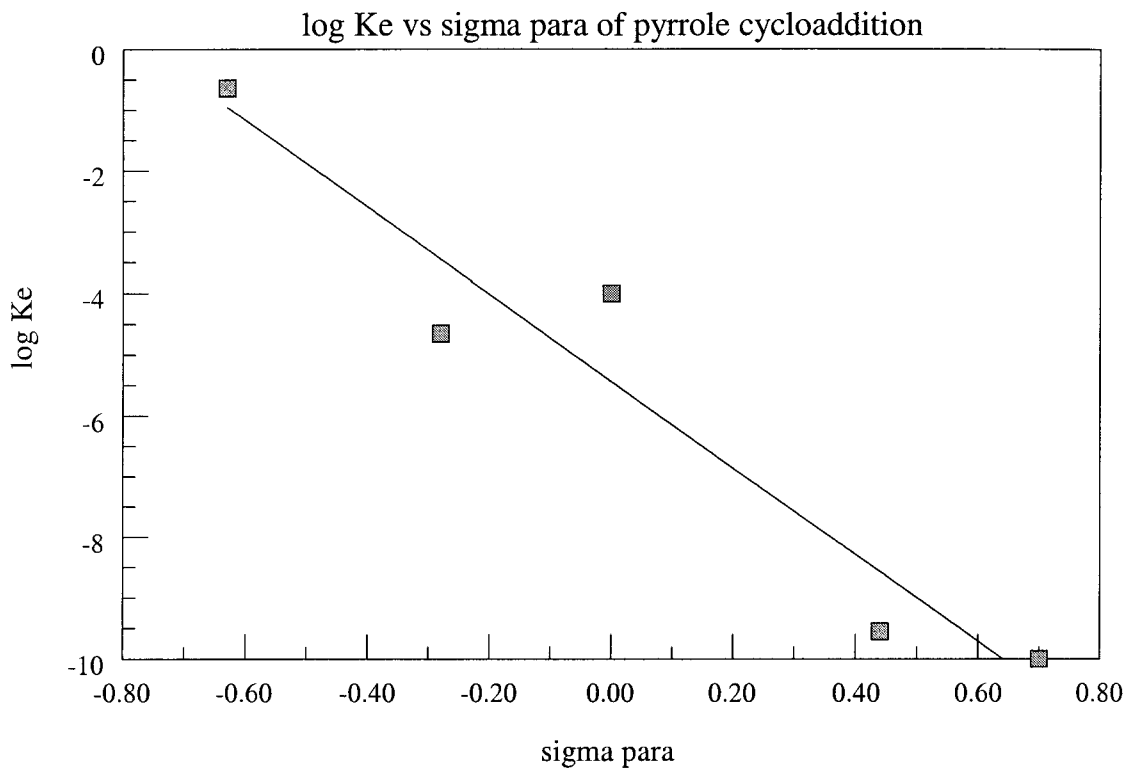


Figure 21: Plot of log Ke of the captioned pyrrole system.

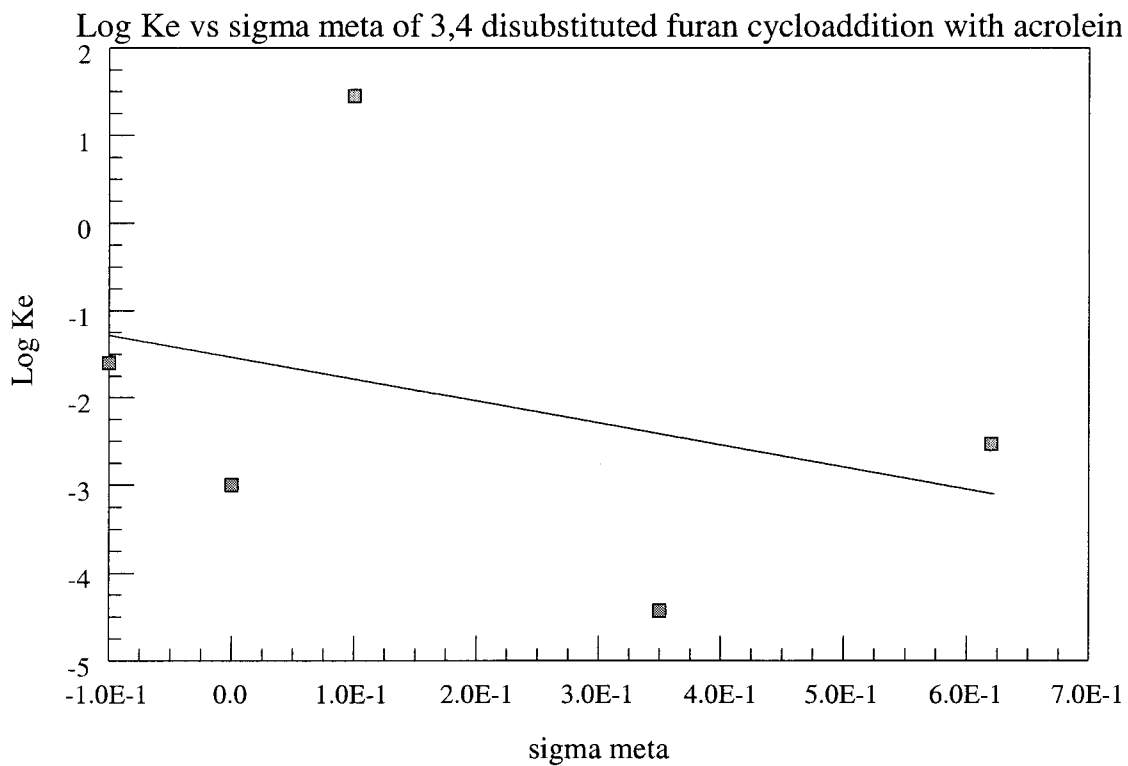


Figure 22: Plot of log Ke of the titled furan system.

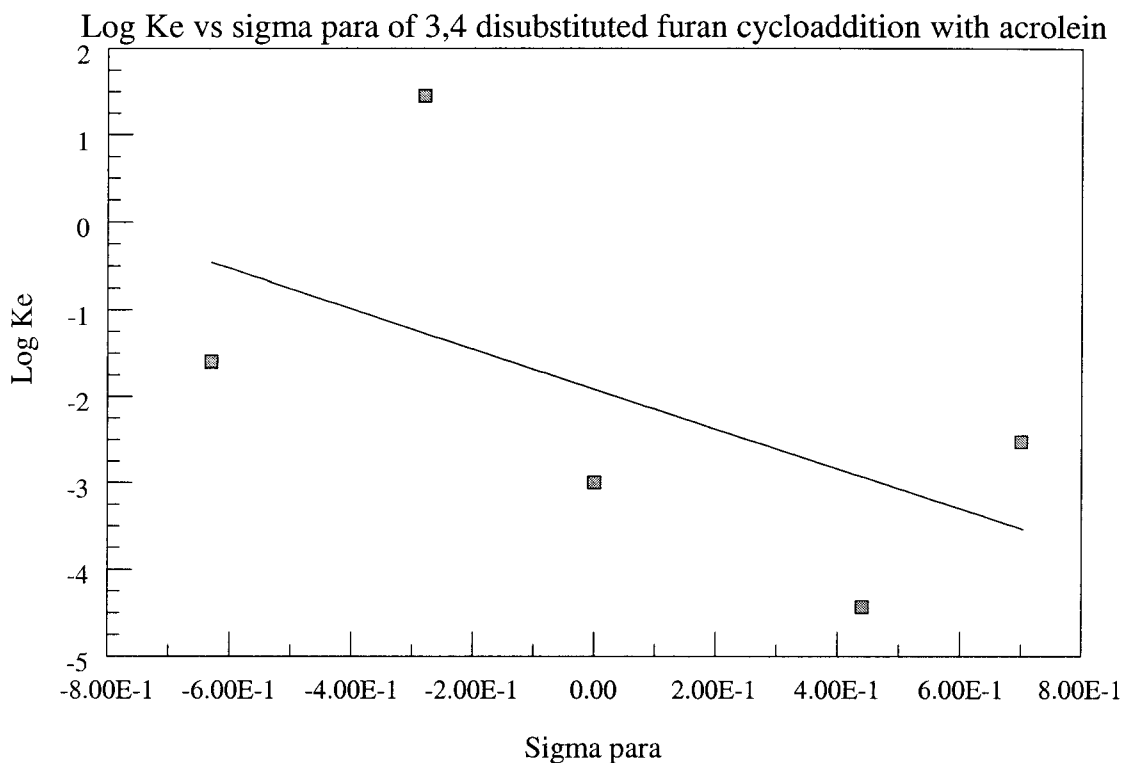


Figure 23: Plot of log Ke of the referenced furan system.

IVE) Correlation between the enthalpy of the Diels-Alder reaction between 3,4 disubstituted furan, thiophene, pyrrole and phosphole vs σ_p and σ_m :

Computed ΔH values usually refer to standard conditions of 298K and 1 bar, and are usually written as ΔH^0 . The superscript is dropped here for convenience. It was found that the enthalpy of the reactions of the four heterocyclic compounds with acrolein are exothermic to different extents, phosphole derivatives reaction with acrolein being the most exothermic followed by furan then by pyrrole and thiophene. It was found also that the enthalpy of these reactions correlates linearly with σ_p and σ_m of diene substituent.

Table 7: A least square summary of the plot of enthalpy of endo reaction between 3,4 disubstituted furan with acrolein vs σ_p and σ_m .

Slope and standard deviation of the plot	ΔH (kcal/mole) Exo	ΔH (kcal/mole) Endo	Substituent	Figure
	-11.06	-11.738	-CN ($\sigma_p = 0.7$) ($\sigma_m = 0.62$)	
	-10.66	-9.048	C(O)OCH ₃ ($\sigma_p = 0.44$) $\sigma_m = 0.35$	
ΔH vs σ_p 3.2+/- 2.3	-12.06	-10.755	H ($\sigma_p = 0$) ($\sigma_m = 0$)	29
ΔH vs σ_m 3.5+/- 2.8	-17.24	-16.018	CH ₃ O- ($\sigma_p = -0.28$) ($\sigma_m = 0.1$)	28
	-15.18	-13.623	N(CH ₃) ₂ ($\sigma_p = -0.63$) ($\sigma_m = -0.1$)	

Table 8: A least square summary of the plot of enthalpy of endo reaction between 3,4 disubstituted phosphole with acrolein vs σ_p and σ_m .

Slope and standard deviation of the plot	ΔH (kcal/mole) Exo	ΔH (kcal/mole) Endo	Substituent	Figure
	-17.22	-18.88	-CN ($\sigma_p = 0.7$) ($\sigma_m = 0.62$)	
	-17.51	-19.403	C(O)OCH ₃ ($\sigma_p = 0.44$) ($\sigma_m = 0.35$)	
ΔH vs σ_p 0.7867+/- 0.5	-18.56	-20.165	H ($\sigma_p = 0$) ($\sigma_m = 0$)	
ΔH vs σ_m 1.79+/- 0.35	-16.78	-19.224	CH ₃ O- ($\sigma_p = -0.28$) ($\sigma_m = 0.1$)	27
	-18.01	-20.268	-N(CH ₃) ₂ ($\sigma_p = -0.63$) ($\sigma_m = -0.1$)	

Table 9: A least square summary of the plot of enthalpy of endo reaction between 3,4 disubstituted pyrrole with acrolein vs σ_p and σ_m .

Slope and standard deviation of the plot	$\Delta H(\text{kcal/mole})$ Exo	$\Delta H(\text{kcal/mole})$ Endo	Substituent	Figure
	-3.07	-1.718	-CN ($\sigma_p = 0.7$) ($\sigma_m = 0.62$)	
	-4.14	-2.63	C(O)OCH ₃ ($\sigma_p = 0.44$) $\sigma_m = 0.35$	
ΔH vs σ_p 5.77+/- 1.48	-7.40	-6.05	H ($\sigma_p = 0$) ($\sigma_m = 0$)	24
ΔH vs σ_m 9.69+/- 2.1	-10.34	-9.45	CH ₃ O- ($\sigma_p = -0.28$) ($\sigma_m = 0.1$)	
	-8.19	-8.03	-N(CH ₃) ₂ ($\sigma_p = -0.63$) ($\sigma_m = -0.1$)	

Table 10: A least square summary of the plot of enthalpy of endo reaction between 3,4 disubstituted thiophene with acrolein vs σ_p and σ_m .

Slope and standard deviation of the plot	$\Delta H(\text{kcal/mole})$ Exo	$\Delta H(\text{kcal/mole})$ Endo	Substituent	Figure
	-2.42	-1.593	-CN ($\sigma_p = 0.7$) ($\sigma_m = 0.62$)	
	-2.32	-1.77	C(O)OCH ₃ ($\sigma_p = 0.44$) $\sigma_m = 0.35$	
ΔH vs σ_p 3.1+/- 0.7	-3.98	-3.541	H ($\sigma_p = 0$) ($\sigma_m = 0$)	25
ΔH vs σ_m 5+/- 1.15	-4.78	-5.428	CH ₃ O- ($\sigma_p = -0.28$) ($\sigma_m = 0.1$)	26
	-4.53	-4.984	-N(CH ₃) ₂ ($\sigma_p = -0.63$) ($\sigma_m = -0.1$)	

Figures 24-29 give plots of ΔH vs σ_p and σ_m of the Diels-Alder reaction between 3,4 disubstituted five membered heterocyclic aromatic rings and acrolein.

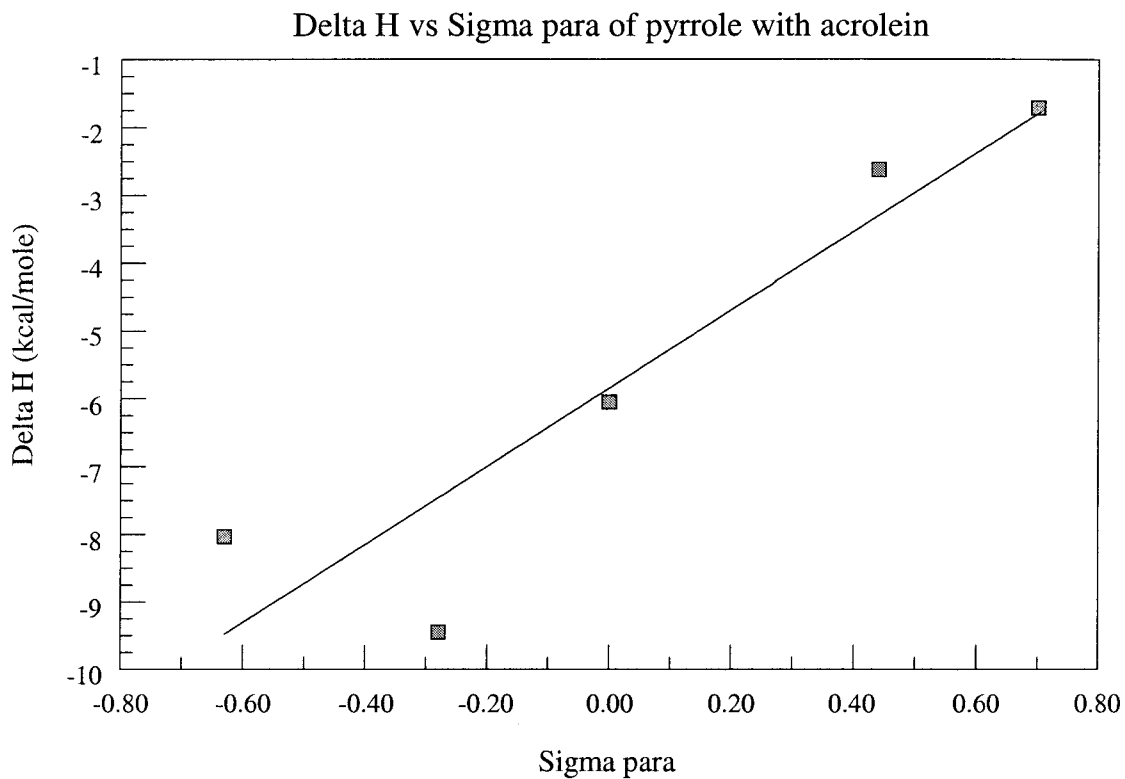


Figure 24: Plot of ΔH of the titled pyrrole system.

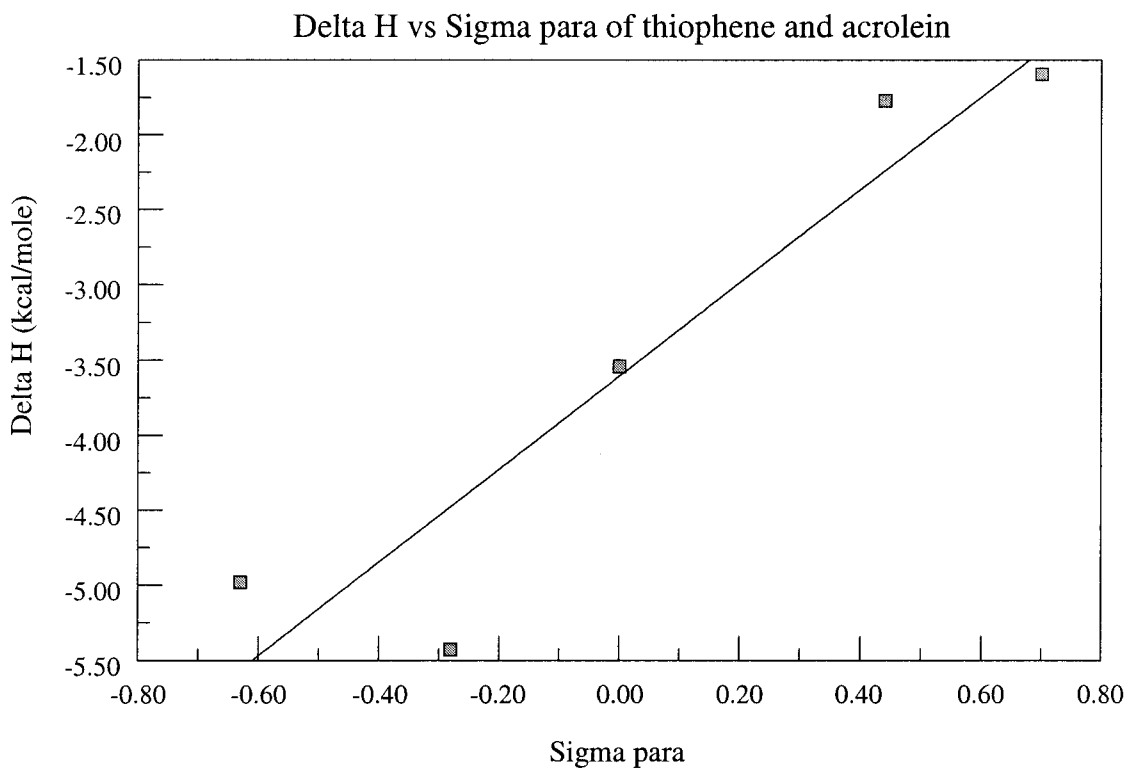


Figure 25: Plot of ΔH of the referenced thiophene system.

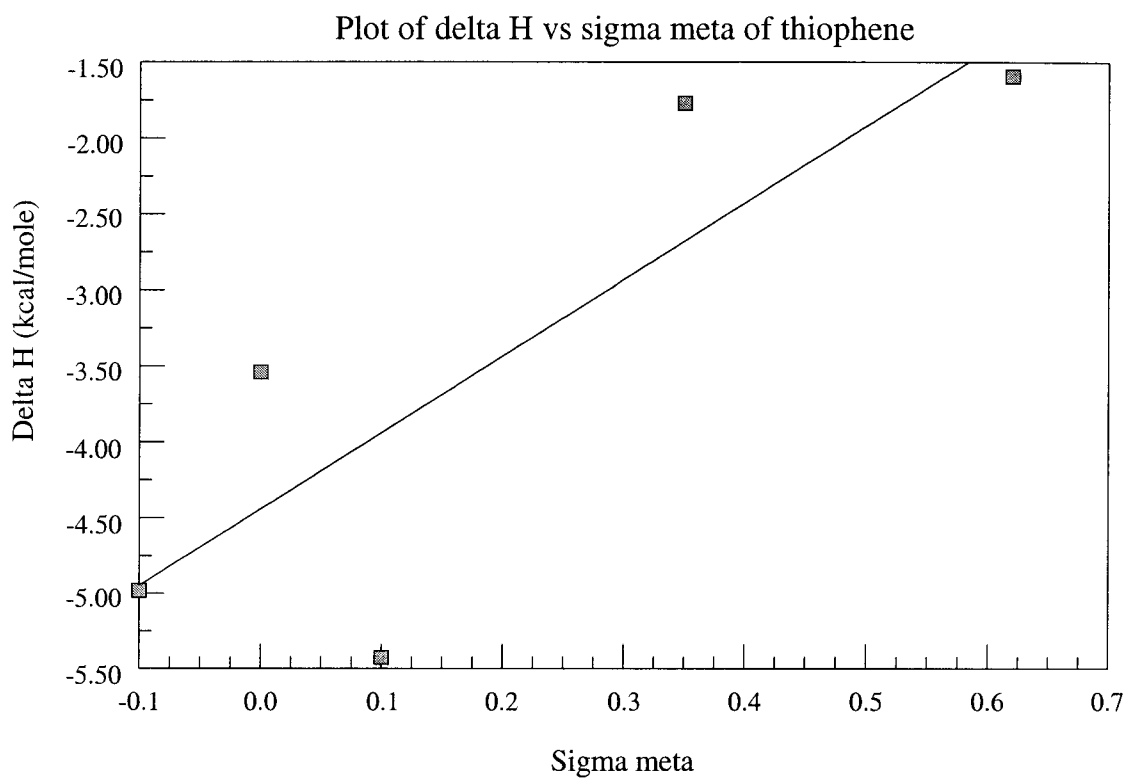


Figure 26: Plot of ΔH of the captioned thiophene system.

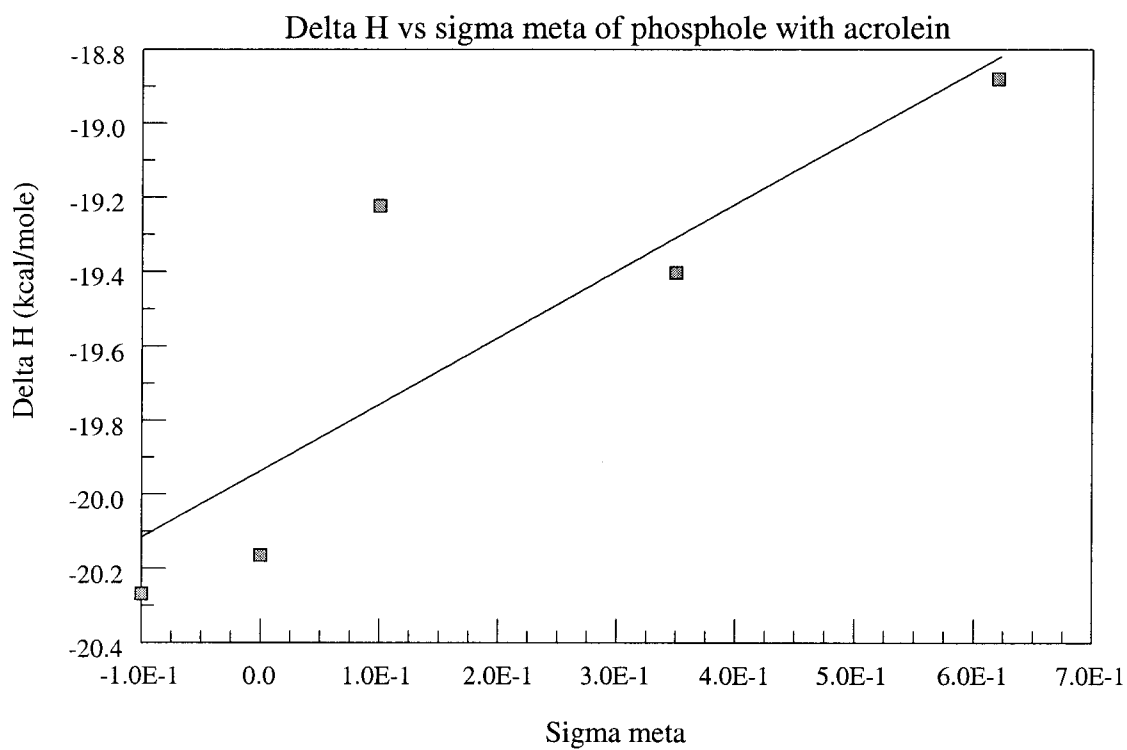


Figure 27: Plot of ΔH of the titled phosphole system.

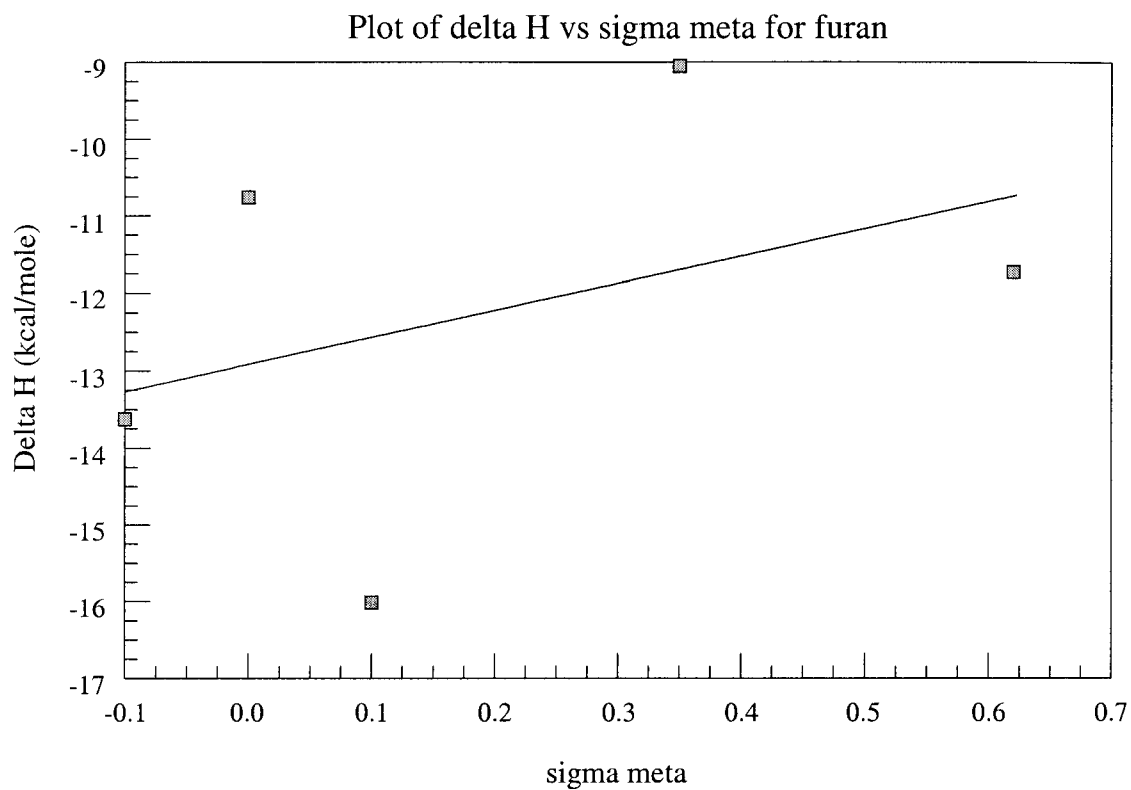


Figure 28: Plot of ΔH of the titled furan system.

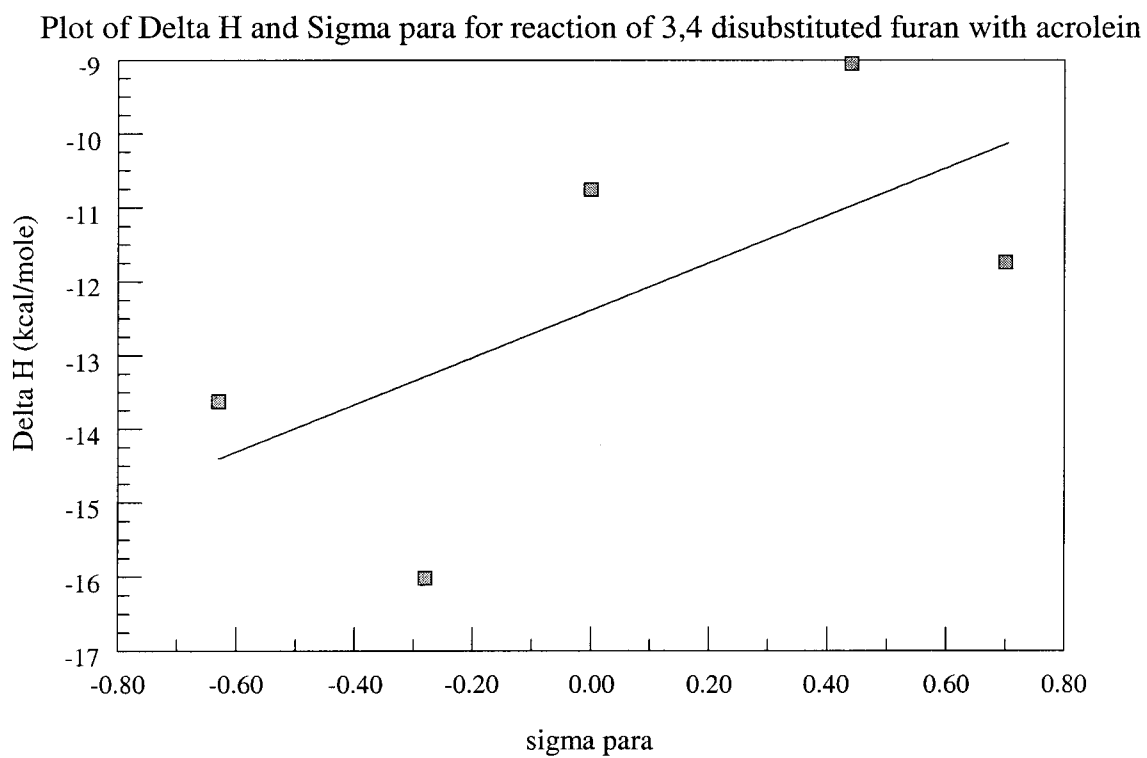


Figure 29: Plot of ΔH of the referenced furan system.

V) Synopsis of kinetic work

The present kinetic study of the Diels-Alder reaction of 3,4 disubstituted furan, thiophene, pyrrole, and phosphole with acrolein using PM3 level of the semi-empirical method gave inconclusive results. Plots of the activation energy of these reactions vs σ_p and σ_m of Hammett equation gave linear correlations with uncertainties larger than the slopes of the lines. Analogous results were obtained when plotting the activation energy of these reactions vs $E_{\text{HOMO}}(\text{diene}) - E_{\text{LUMO}}(\text{dienophile})$. Our explanation for this is that the activation energy can be influenced to a certain degree by the steric repulsion in the transition state between the carbonyl group of acrolein and the bulky substituents on the diene. A second factor is that the transition state orbitals are by their nature more diffuse, due to bond deformation. Since AM1 and PM3 are parametrized for stable ground state molecules with less diffuse orbitals, these models can't be expected to accurately reflect transition state energies. Tables 11 through 14 give computed values for the activation energies of the different Diels-Alder reactions as a function of the substituent on the diene (computed using PM3 method).

Table 11: Activation energy(kcal/mol) of endo Diels-Alder reaction of 3,4 disubstitued furan with acrolein.

Substituent	Activation energy (kcal/mol)	$E_{\text{HOMO}} - E_{\text{LUMO}}$(kcal/mol)
H	33.5	-211.1
Dicyano	35.1	-233.9
Formic acid-dimethyl ester	36.6	-230.2
Dimethoxy	31.3	-206.7
Dimethylamine	32.1	-194.7

Table 12: Activation energy(kcal/mol) of endo Diels-Alder reaction of 3,4 disubstituted thiophene with acrolein.

Substituent	Activation energy (kcal/mol)	$E_{\text{HOMO}} - E_{\text{LUMO}}$ (kcal/mol)
H	48	-208.8
Dicyano	51.2	-227.77
Formic acid dimethyl ester	48.5	-227.83
Dimethoxy	47.95	-193.5
Dimethylamine	47.92	-185.5

Table 13: Activation energy(kcal/mol) of endo Diels-Alder reaction of 3,4 disubstituted pyrrole with acrolein.

Substituent	Activation energy (kcal/mol)	$E_{\text{HOMO}} - E_{\text{LUMO}}$ (kcal/mole)
H	41.6	-195.9
Dicyano	47	-220.3
Formic acid-dimethyl ester	45.4	-216.8
Dimethoxy	41.3	-193.7
Dimethylamine	42.2	-193

Table 14: Activation energy(kcal/mol) of endo Diels-Alder reaction of 3,4 disubstituted phosphole with acrolein.

Substituent	Activation energy (kcal/mol)	$E_{\text{HOMO}} - E_{\text{LUMO}}$ (kcal/mol)
H	42.9	-212.9
Dicyano	44.1	-232.3
Formic acid-dimethyl ester	43.4	-229.5
Dimethoxy	42.3	-202
Dimethyl amine	41.5	-200

Tables 15 and 16 give least square summaries of the plots of the activation energy of the Diels-Alder reaction of 3,4 disubstituted furan, thiophene, pyrrole, and phosphole with vs σ_R of Taft equation and vs $[E_{\text{HOMO}}(\text{diene}) - E_{\text{LUMO}}(\text{dienophile})]$ respectively.

Table 15: A least square summary of the plots of the activation energy of the Diels-Alder reaction of 3,4 disubstituted furan, thiophene, pyrrole, and phosphole vs σ_R of Taft equation.

System	Slope and standard deviation of the line
Furan	1.5+/-2.4
Thiophene	3.16+/- 1.3
Pyrrole	2.8+/- 2.8
Phosphole	2.2+/- 0.9

Table 16: A least square summary of the plots of the activation energy of the Diels-Alder reactions of furan, thiophene, pyrrole, and phosphole with acrolein vs ($E_{HOMO} - E_{LUMO}$).

System	Slope and standard deviation of the line
Furan	-0.11+/- 1.24
Thiophene	-0.05+/- 1.2
Pyrrole	-0.2+/- 0.6
Phosphole	-0.06+/- 0.4

Except for phosphole the deviations in the slopes exceed the slope values themselves, showing no good correlation exists using PM3. The phosphole systems result of a successful correlation vs σ_R and (not $E_{HOMO} - E_{LUMO}$ gap) is related to the greater reactivity of the group, and hence sensitivity to the substituent, as shown by the phosphole's having the only equilibrium constants exceeding unity.

Figure 30 is a representative energy profile for the retro-Diels-Alder reaction of 3,4 disubstituted furan with acrolein:

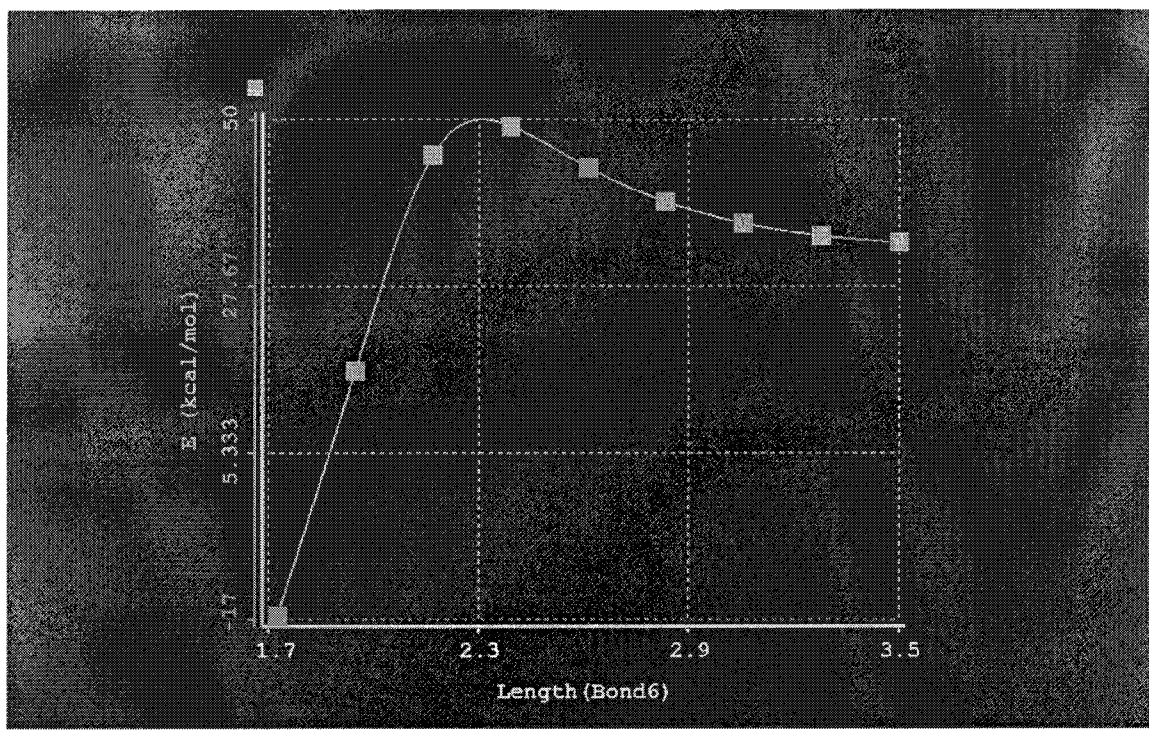


Figure 30: Energy profile for the endo retro-Diels-Alder reaction of 3,4 disubstituted furan with acrolein.

Figure 31 is a representative plot of the activation energy E_a of the endo Diels-Alder reaction of 3,4 disubstituted furan with acrolein vs σ_R of Taft equation.

$$\text{Log } k = \text{log } k_0 + \rho\sigma_R$$

where k , k_0 are rate constants of the substituted and non substituted system respectively, σ_R is Taft equation resonance contribution of the substituent and ρ is the slope of the line.

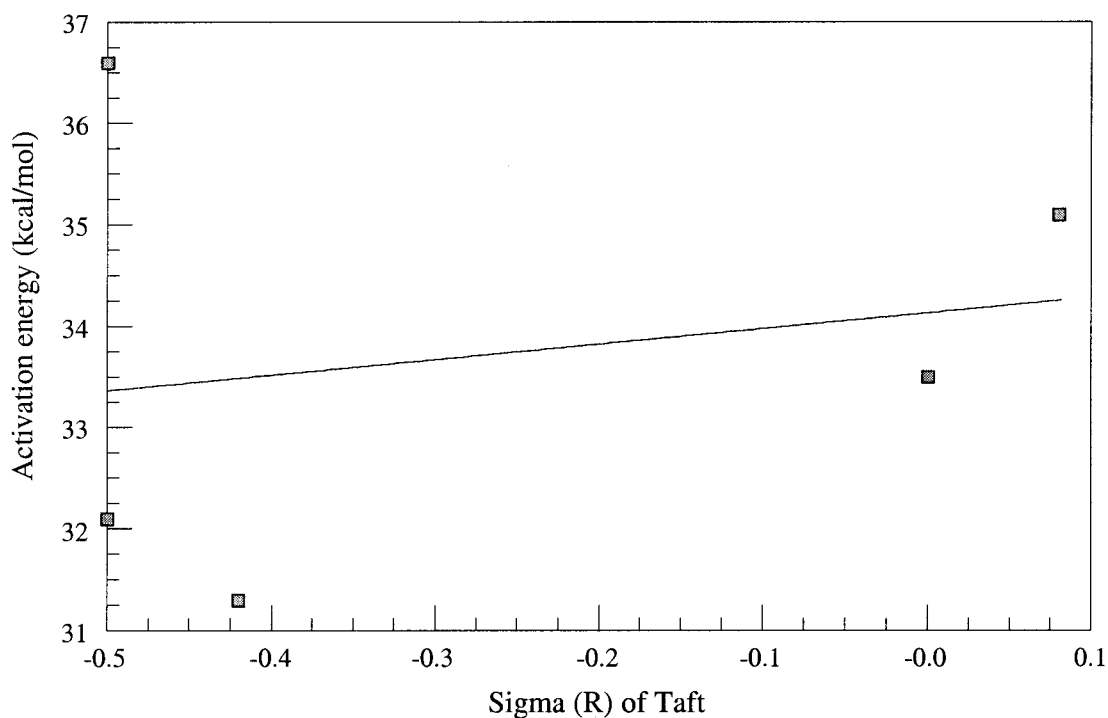


Figure 31: Plot of the activation energy of retro-Diels-Alder reaction of 3,4 disubstituted furan with acrolein vs σ_R of Taft equation.

It is clear from Table 15 that even if the Taft σ_R are used (more traditional for kinetic study), there is still no correlation using PM3 model, except for the phosphole systems as noted.

VI) Future work

As a next step we would like to investigate the kinetics of the Diels-Alder reaction between 3,4 disubstituted N, P, O and S substituted 5-membered heterocyclic aromatic compounds with acrolein. It was found by Houk³¹ that the best computational method for predicting the energy of the transition state of the Diels-Alder reaction is B3LYP of the Density Functional Theory, this is perhaps due to the added flexibility of the DFT in modeling more diffuse transition states. Our previous calculations for the transition state energy of the Diels-Alder reaction (Scheme 8) using semi-empirical AM1 and PM3 gave inconclusive results. We will try to find correlations between activation energy of the Diels-Alder reaction and σ_R of Taft equation. We expect that electron donating groups will raise the energy of the HOMO of the diene. This, in turn, is expected to lower the activation barrier. Next we will plot the activation energy against the energy difference between the HOMO of the diene (heterocyclic ring) and the LUMO of the dienophile (acrolein). In this case also we expect a linear correlation. In addition we would like to plot the activation energy of the Diels-Alder reaction vs E_{HOMO} and E_{LUMO} of the diene. We expect that these correlations will be linear, because the energy of both the HOMO and LUMO of the diene are raised with electron donating substituents, which thereby lowers the activation energy of the reaction.

VII) Conclusions

This project is the first to compare computed and experimental enthalpy and equilibrium constants of Diels-Alder reactions of N, P, O and S substituted heterocyclic 5-membered aromatic rings with acrolein. The method, results and conclusions of this project have recently been published.³² The literature review conducted for these compounds gave no results for reactions with acrolein, but other dienophiles reacted successfully. The conclusion we draw from the literature review is that these heterocyclic compounds can indeed undergo the Diels-Alder reactions. A conclusion we can draw from our work is that all four heterocyclic compounds behave like dienes to different degrees, and the reactions with furan are more exothermic than with pyrrole, perhaps because the energy level of the HOMO of furan is higher than that of pyrrole. Another possible explanation of this trend is that oxygen in furan is more electronegative than the nitrogen in pyrrole, which makes pyrrole more aromatic (and hence more stable) than furan, so furan behaves like a less stable butadiene. Likewise pyrrole is still less reactive than phosphole because it is more aromatic. This can be explained by realizing that the valence p-orbital on phosphorus is larger than the corresponding p-orbital on nitrogen, which makes the overlap of the π system of the aromatic ring in phosphole less effective, and this in turn destabilizes the HOMO of phosphole more than the HOMO of pyrrole. It is also important to note that phosphole is 8° out of plane (our PM3 calculation), and hence less aromatic for this reason also.

Thiophene and pyrrole were found to be unreactive dienes because of the low exothermicities of their reactions with acrolein, though both are aromatic to some extent with pyrrole being more so. This difference is due to a more diffuse p orbital on sulfur.

Furan is not a very good aromatic compound because the oxygen in furan is very electronegative which localizes its nonbonding electron pair.

Another noteworthy observation is that the HOMO and LUMO energies of the diene correlate linearly with σ_p and σ_m of Hammett equation. This means that the known electron donating and electron withdrawing effects of these groups change the energy levels of the HOMO and LUMO orbitals of the dienes in a linear manner.

Another observation is that the log of the equilibrium constant of the Diels-Alder reaction of the four heterocyclic compounds with acrolein correlates linearly with σ_p and σ_m of Hammett equation. This means that the value of the equilibrium constant is sensitive to electron donating and electron withdrawing groups on the heterocyclic rings. A related conclusion is that the enthalpy of the Diels-Alder reactions correlates linearly with σ_p and σ_m . The more electron donating the substituent on the diene, the larger the exothermicity of the reaction.

Although $\log K_e$, $E_{\text{HOMO}}(\text{diene})$ and ΔH correlate favourably with σ_p or σ_m , no reasonable correlation results when they are plotted against themselves. That is, except for $\log K_e$, (which is calculated from ΔH and ΔS), $\log K_e$ and $E_{\text{HOMO}}(\text{diene})$ do not correlate well with each other. This is because the individual error each parameter experiences when plotted vs σ_p or σ_m is compounded when they are plotted against each other. Thus PM3 level of treatment for these systems is sufficient to correlate the electron donating effects vs any directly connected parameters. However, it is not sufficiently precise to correlate relationships among parameters indirectly linked to each other through the substituent effect

VIII) Bibliography

- 1) Diels, O. and Alder, K. *Liebigs Ann. Chem.* **1928**, 98, 460.
- 2) Sauer, J. and Sustmann, R. *Angew. Chem. Int. Ed. Engl.* **1980**, 19, 779.
- 3) Reinhoudt, D. N. and Kouwenhoven, C. G. *Tetrahedron*, **1974**, 30, 2093.
- 4) Bosshand, P. and Eugster, C. H. *Adv. Heterocycl. Chem.* **1966**, 7, 377.
- 5) Mandell, L. and Blanchard, W. A. *J. Am. Chem. Soc.* **1957**, 79, 6198.
- 6) Lelievre, S.; Mercier, F. and Mathey, F. *J. Org. Chem.* **1996**, 61, 3531.
- 7) Mele, B. V. and Huybrechts, G. *Int. J. Chem. Kinetics*, **1989**, 21, 967.
- 8) Mele, B. V.; Tybaert, C. and Huybrechts, G. *Int. J. Chem. Kinetics*, **1987**, 19, 1063.
- 9) Huybrechts, G.; Leemans, W. and Mele, B. V. *Int. J. Chem. Kinetics*, **1982**, 14, 997.
- 10) Cetiviela, C.; Mayoral, A.; Avenoza, A.; Peregrina, J. M. and Roy, M. A. *J. Phys. Org. Chem.* **1990**, 3, 414.
- 11) Wasserman, A. *Diels-Alder reactions*, Elsevier Pub. Co., 1965.
- 12) Jursic, B. *Theochem.* **1998**, 454, 105-116
- 13) Vijaya, R. ; Dinadayalana, T. C. and Narahari, G. *Theochem.* **2002**, 589-590, 291-299.
- 14) Fu, Y. S.; Tsai, S. C.; Huang, C. H.; Yen, S. Y.; Hu, W. P. and Yu, S. J. *J. Org. Chem.* **2003**, 68, 3068.
- 15) Wasserman, A. *J. Chem. Soc.* **1935**, 828.
- 16) A) Littman, E. R. *J. Am. Chem. Soc.* **1936**, 58, 1316.
B) Kistiakowsky, G. B. and Mears, W. H. *J. Chem. Phys.* **1937**, 5, 680.

- 17) Fukui, A. and Fujimoto, N. *Bull. Chem. Soc. Jpn.* **1967**, *40*, 2018.
- 18) Fringuelli, F.; Minuti, L.; Pizzo, F. and Taticchi, A. *Acta. Chem. Scand.* **1993**, *47*, 255.
- 19) Bodwell, G. J. and Pi. Z. *Tetrahedron Lett.* **1997**, *38*, 309.
- 20) Li, Y. and Houk, K. N. *J. Am. Chem. Soc.* **1993**, *115*, 7478.
- 21) Yates, P. and Eaton, P. J. *J. Am. Chem. Soc.* **1960**, *82*, 4436.
- 22) Hehre, W. J.; Ditchfield, R. and Pople, J. A. *J. Chem. Phys.* **1972**, *56*, 2257.
- 23) Binkley, J. S.; Pople, J. A. and Hehre, W. J. *J. Chem. Soc.* **1980**, *102*, 939.
- 24) Hariharan, P. C. and Pople, J. A. *Chem. Phys. Lett.* **1972**, *66*, 217.
- 25) Balbi, N. and Khoumeri, B. *J. Thermal Anal.* **1994**, *42*, 461.
- 26) A) Parr, R. G. and Yang, W. *Density Functional Theory of Atoms and Molecules*, Oxford Univ. Press, 1989. B) Becke, A. D. *J. Chem. Phys.* **1993**, *98*, 1372. C) Pederson, T. B. www.fysik.dtu.dk/Bligaard/ms/node8.html, (accessed 7/22/2003).
- 27) Stewart, J. J. P. *J. Computational Chem.* **1989**, *10*, 209.
- 28) Hehre, W. J.; Stewart, R. F. and Pople, J. A. *J. Chem. Phys.* **1996**, *51*, 2657.
- 29) Khoumeri, B.; Balbi, N.; Balbi, J. H.; Bighelli, A.; Temi, F. and Casanova J. *Thermochem. Acta.* **1995**, *259*, 121.
- 30) Rogers, F. E. *J. Phys. Chem.* **1971**, *75*, 1734-1737
- 31) Houk, K. N. and Evanseck, J. D. *Angew. Chem. Int. Ed. Engl.* **1992**, *31*, 682 and references therein.
- 32) Musslimani, T. H. and Mettee, H. *Theochem.* **2004**, *672*, 35-43.